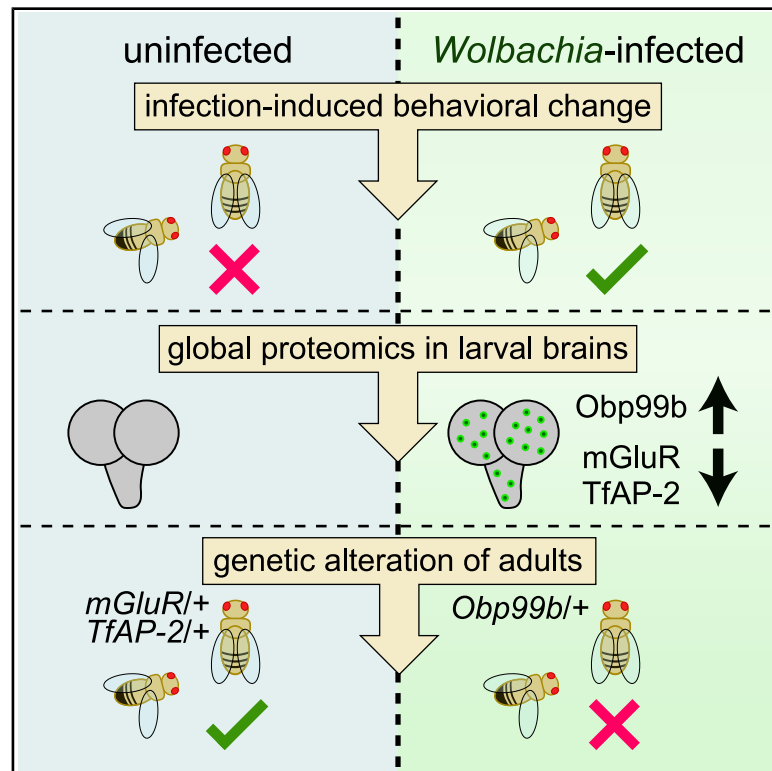


Wolbachia-mediated reduction in the glutamate receptor mGluR promotes female promiscuity and bacterial spread

Graphical abstract



Authors

Brandt Warecki, Giovanni Vega, Sommer Fowler, Grant Hartzog, Timothy L. Karr, William Sullivan

Correspondence

bwarecki@ucsc.edu (B.W.), tkarr@asu.edu (T.L.K.)

In brief

The mechanisms by which parasites mediate host behavioral changes remain largely unexplored. Warecki et al. describe a molecular mechanism for how the endosymbiont *Wolbachia* induces increased mating in female *Drosophila*: neuronal reduction of the metabotropic glutamate receptor mGluR.

Highlights

- *Wolbachia* infection increases female receptivity to mating in *Drosophila*
- *Wolbachia* colonize regions of the female brain important for mating
- mGluR among proteins reduced in abundance in infected female brains
- Genetic reduction of mGluR phenocopies *Wolbachia* infection

Article

Wolbachia-mediated reduction in the glutamate receptor mGluR promotes female promiscuity and bacterial spread

Brandt Warecki,^{1,4,*} Giovanni Vega,¹ Sommer Fowler,¹ Grant Hartzog,¹ Timothy L. Karr,^{2,3,*} and William Sullivan^{1,3}

¹Department of Molecular, Cell, and Developmental Biology, University of California, Santa Cruz, Santa Cruz, CA 95064, USA

²ASU-Banner Neurodegenerative Disease Research Center, Biodesign Institute, Arizona State University, Tempe, AZ 85287, USA

³Senior author

⁴Lead contact

*Correspondence: bwarecki@ucsc.edu (B.W.), tkarr@asu.edu (T.L.K.)

<https://doi.org/10.1016/j.celrep.2025.115629>

SUMMARY

The molecular mechanisms by which parasites mediate host behavioral changes remain largely unexplored. Here, we examine *Drosophila melanogaster* infected with *Wolbachia*, a symbiont transmitted through the maternal germline, and find *Wolbachia* infection increases female receptivity to male courtship and hybrid mating. *Wolbachia* colonize regions of the brain that control sense perception and behavior. Quantitative global proteomics identify 177 differentially abundant proteins in infected female larval brains. Genetic alteration of the levels of three of these proteins in adults, the metabotropic glutamate receptor mGluR, the transcription factor TfAP-2, and the odorant binding protein Obp99b, each mimic the effect of *Wolbachia* on female receptivity. Furthermore, >700 *Wolbachia* proteins are detected in infected brains. Through abundance and molecular modeling analyses, we distinguish several *Wolbachia*-produced proteins as potential effectors. These results identify potential networks of host and *Wolbachia* proteins that modify behavior to promote mating success and aid the spread of *Wolbachia*.

INTRODUCTION

Many parasites alter their hosts' behavior in surprising ways.^{1–3} For example, *Toxoplasma gondii* reduces rodents' fear of predation,⁴ and the fungus *Entomophthora muscae* induces *Drosophila* to climb upward before their death.⁵ However, the molecular mechanisms governing behavioral alterations are unclear. Because some behavioral alterations aid the transmission of the parasite, alteration of host behavior is often viewed as an adaptive strategy employed by the parasite to promote its own spread^{6,7} and has been referred to as an “extended phenotype” of the parasitic genome.⁸ However, host behavioral modifications likely rely on complex interactions involving both the host nervous system and immune response to infection.^{9–11} Therefore, understanding the molecular mechanisms that lead to altered behavior is critical to determine if the behavioral change is induced by the parasite or rather a secondary effect of infection.

The endosymbiont bacterium *Wolbachia pipientis* provides a great opportunity for studying host-parasite interactions.¹² *Wolbachia* infect many insect species, including mosquitoes and *Drosophila*^{13,14} and are capable of directly altering host processes by induced host protein expression¹⁵ and the secretion of *Wolbachia*-produced effector proteins.¹⁶ *Wolbachia* colonize both germline and somatic tissues, including the brain.^{17–20} Broadly, *Wolbachia* have direct implications for human health

due to *Wolbachia*'s ability to suppress viral titer in their insect hosts and by suppressing insect populations when introduced to naturally uninfected populations.^{21–25} As such, *Wolbachia* are currently being used to combat viral insect-borne diseases such as dengue and Zika.^{24,26,27}

Wolbachia are primarily inherited by vertical transmission through the maternal germline^{28,29} (reviewed in Kaur et al.^{30,31} and Russell et al.^{30,31}). Therefore, *Wolbachia*-induced manipulations of host reproduction that increase the relative fitness of infected females, such as cytoplasmic incompatibility and increased female fertility, promote the spread of *Wolbachia* through populations.^{32,33} Additionally, *Wolbachia* are capable of horizontal transmission between species.^{34–38} Horizontal transmission occurs through a variety of potential mechanisms,^{34,39,40} including hybrid mating and subsequent introgression.^{41,42}

Interestingly, maternal *Wolbachia* infection may lead to increased hybrid mating between the closely related *Drosophila melanogaster* and *D. simulans* species.⁴³ *Wolbachia* infection has been proposed to alter host activity and behavior in processes important for sense perception, courtship, and mating.^{2,44–58} However, a role for *Wolbachia* in *D. melanogaster* and *D. simulans* assortative mating has not been observed.^{59,60} In some cases, behavioral modifications may be correlated with *Wolbachia* infection in the developing and adult brain.¹⁸ However, the mechanisms by which *Wolbachia* alter host behavior remain unknown.

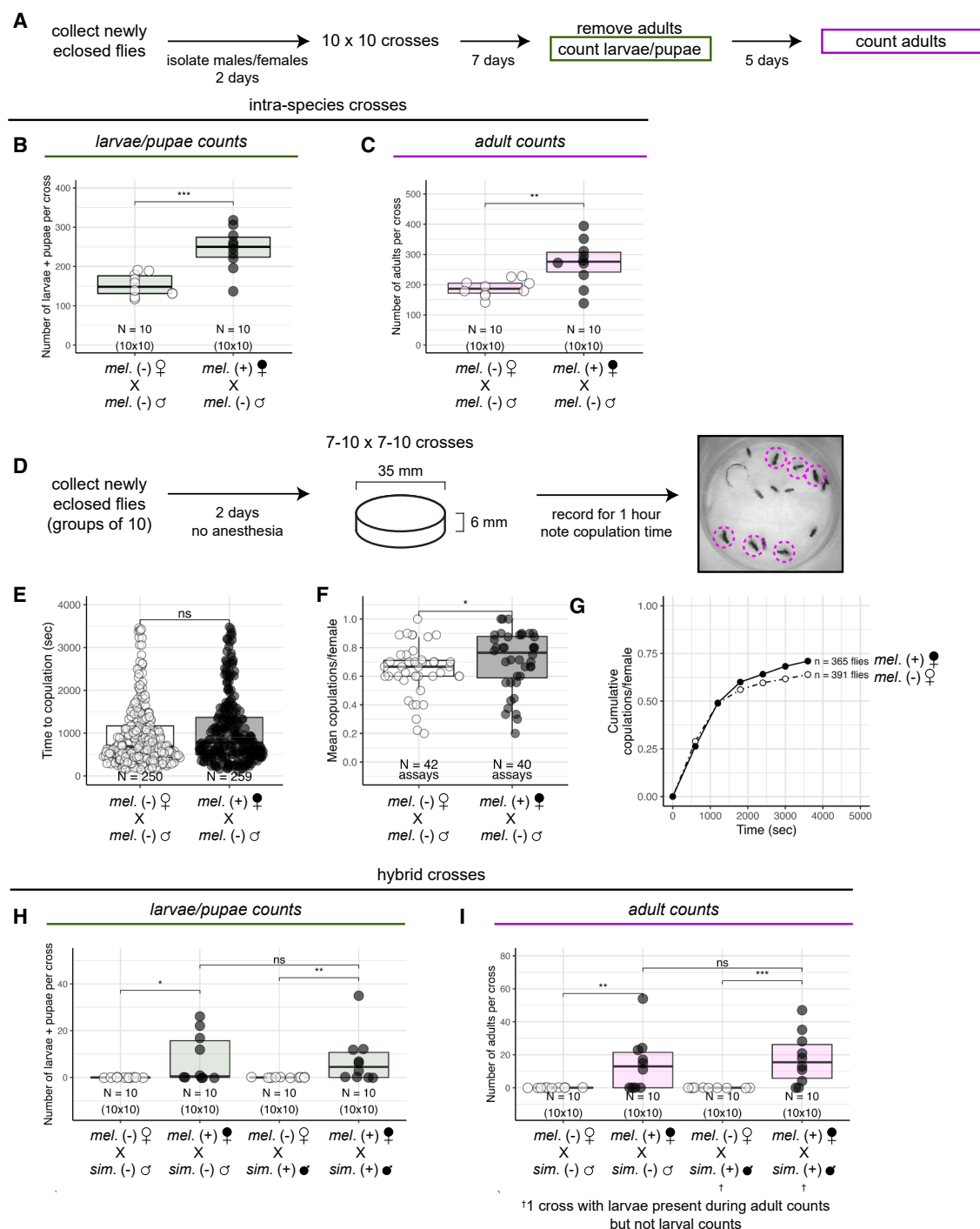


Figure 1. *Wolbachia* increases the receptivity of female *D. melanogaster* to mating

(A) Ten 2-day-old females were crossed with ten 2-day-old males for 7 days at which point adults were removed and crawling third instar larvae and pupae were counted. After a further 5 days, emerged adults were counted.

(B and C) The total number of larvae + pupae (B) and the total number of adults (C) collected from crosses with uninfected (white symbols and dots) and infected (black symbols and dots) *D. melanogaster* females crossed to uninfected *D. melanogaster* males. Each dot represents the progeny from one 10 × 10 cross. Data are represented as median +/− upper and lower quartiles. ***p* < 0.01, ****p* < 0.001 by two-sided Mann-Whitney tests.

(D) Seven to ten 2-day-old female flies were placed in a mating chamber with seven to ten 2-day-old male flies and filmed for 1 h

(legend continued on next page)

Here, we examined the molecular mechanisms by which *Wolbachia* infection alters mating behavior in *D. melanogaster* females. We found that *D. melanogaster* females were generally more receptive to mating when infected with *Wolbachia* for both intra-species and hybrid crosses, consistent with previous results.⁴³ To investigate how *Wolbachia* mediate these behavioral alterations, we performed mass spectrometry-based global proteomics and label-free quantitation to identify 177 differentially abundant proteins between uninfected and *Wolbachia*-infected female larval brains. Among these, genetic alterations of the dosages of mGluR (metabotropic glutamate receptor), Obp99b (odorant-binding protein 99b), and TlAP-2 (transcription factor AP-2) in adults phenocopied to different degrees the presence/absence of *Wolbachia* in uninfected/infected female flies, respectively. Additionally, we identified several *Wolbachia* proteins that may act as effectors to disrupt eukaryotic pathways in the brain.

Collectively, these results provide a molecular basis for an observed behavioral effect promoted by *Wolbachia* infection in the brain. Through modification of neurotransmission and sense perception, *Wolbachia* increase female receptivity, which contributes to increased progeny yields that can provide a driving force for the spread of *Wolbachia* into new populations.

RESULTS

Wolbachia infection is correlated with increased female receptivity to both intra-species and hybrid mating

In *Drosophila*, *Wolbachia* increase the relative fitness of infected females through several mechanisms that subsequently promote *Wolbachia* transmission through a population. The mechanisms utilized by *Wolbachia* involve both behavioral and physiological alterations to the host, including increased fertility and fecundity of *D. melanogaster* females,^{32,61} and possibly increased female receptivity.⁴³

To measure the consequences of *Wolbachia*-induced changes to the reproductive success of *D. melanogaster*, we compared the numbers of progeny recovered from 10 × 10 crosses between *Wolbachia*-infected and uninfected flies (Figure 1A, see STAR Methods). We measured both larval and adult progeny to reflect the fact that larval counts were not a total sum of the progeny produced but only those visible 7 days after the cross was performed. An increased number of adults collected from these crosses, which provides a more thorough count, indicates that mating occurred at an increased rate. For crosses between *D. melanogaster* females and uninfected

males, we observed a statistically significant increase in the number of larvae produced from *Wolbachia*-infected females (mean = 245 SD = 53 per 10 × 10 cross, *N* = 10) compared with uninfected females (mean = 153 SD = 28 per 10 × 10 cross, *N* = 10; *p* = 3.2 × 10^{−4} by Mann-Whitney test) (Figure 1B). We observed a similar increase in the number of adults from infected females (mean = 273 SD = 75 per 10 × 10 cross, *N* = 10) compared with uninfected females (mean = 189 SD = 28 per 10 × 10 cross, *N* = 10; *p* = 9.1 × 10^{−3} by Mann-Whitney test) (Figure 1C). Thus, female *Wolbachia* infection provides a reproductive advantage for *D. melanogaster* during this time frame.

We determined if the increased progeny we recovered from crosses involving *Wolbachia*-infected females were associated with alterations in mating behavior. We directly observed grouped mating assays (see STAR Methods) and determined if female *Wolbachia* infection altered mating time or success (Figure 1D). We observed no decrease in the time to copulation for infected females compared with uninfected females (Figure 1E). However, there was a slight but significant increase in the average number of copulations per female when females were infected with *Wolbachia* (*p* = 0.034 by Mann-Whitney test; Figure 1F). As this difference in copulation rate was smaller than the differences in progeny produced between infected and uninfected females, the increased progeny from crosses with infected females can only partially be explained through increased mating. However, while this measured difference was small, modeling *Wolbachia* spread through a population using only the measured copulation rates (Figure S1A) suggested that this increased copulation could contribute to driving *Wolbachia* spread at an increased rate (Figure S1B). Comparing the overall number of copulations per female over time between infected and uninfected females revealed the *Wolbachia*-induced increase in copulation success occurred largely toward the end of the mating assays when the copulation rate of uninfected females began to plateau (Figure 1G). Previous experiments indicated that *Wolbachia* infection does not increase the attractiveness of infected females.⁶⁰ Therefore, similar to increased mating in *Wolbachia*-infected *Drosophila* males,⁴⁶ our results suggest *Wolbachia* infection is correlated with increased female receptivity to mating.

To further probe *Wolbachia*'s effect on female receptivity, we examined hybrid crosses between *D. melanogaster* females with *D. simulans* males where *Wolbachia* have previously been reported to promote mating.⁴³ We set up 10 × 10 hybrid crosses between *Wolbachia*-infected and uninfected *D. melanogaster* females and uninfected *D. simulans* males. For hybrid crosses, we observed no larval progeny from crosses involving uninfected

(E) Comparison between the measured times to copulation for uninfected (white dots) and infected (black dots) *D. melanogaster* females presented with uninfected *D. melanogaster* males. Data are represented as median +/− upper and lower quartiles. Each dot represents one successful copulation. ^{ns}*p* > 0.05 by one-sided Mann-Whitney test.

(F) Comparison between the measured copulation rates for uninfected (white dots) and infected (black dots) *D. melanogaster* females presented with uninfected *D. melanogaster* males. Data are represented as median +/− upper and lower quartiles. Each dot represents the percentage of females that copulated during one mating assay. **p* < 0.05 by one-sided Mann-Whitney test. See also Figure S1.

(G) Comparison between the percentage of total females that copulated over time for uninfected (white dots) and infected (black dots) *D. melanogaster* females presented with uninfected *D. melanogaster* males.

(H and I) The numbers of larvae + pupae (H) and adults (I) collected from crosses with uninfected (white dots) and infected (black dots) *D. melanogaster* females crossed to uninfected (white symbols) and infected (black symbols) *D. simulans* males. Each dot represents the progeny from one 10 × 10 cross. Data are represented as median +/− upper and lower quartiles. ^{ns}*p* > 0.05, **p* < 0.05, ***p* < 0.01, ****p* < 0.001 by two-sided Mann-Whitney tests.

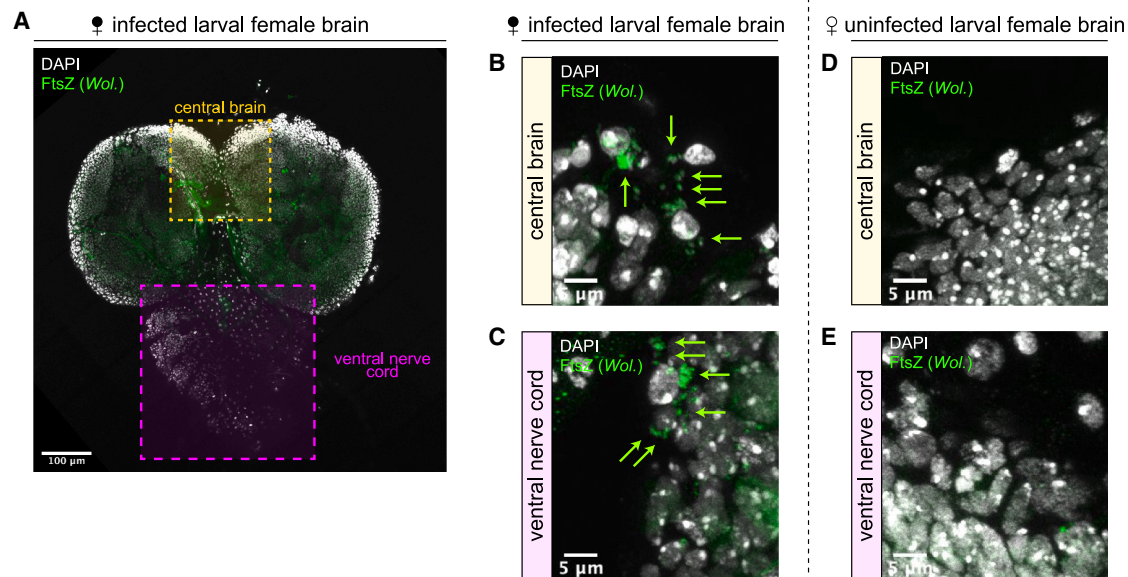


Figure 2. *Wolbachia* colonize the central brain and ventral nerve cord regions of female *D. melanogaster* larval brains

(A) Female larval brain stained with the anti-bacterial antibody FtsZ (green) and DAPI (gray). Scale bar, 100 μ m.

(B and C) FtsZ-stained *Wolbachia* puncta (green arrows) are routinely observed in the central brain (B) and ventral nerve cord (C) regions of infected brains. Scale bars, 5 μ m.

(D and E) No FtsZ-stained puncta are observed in the central brain (D) or ventral nerve cord (E) regions of uninfected brains. Scale bars, 5 μ m.

females (mean = 0 SD = 0 per 10 \times 10 cross, N = 10; Figure 1H) under our experimental conditions. In contrast, we repeatedly observed larval progeny from hybrid crosses involving *Wolbachia*-infected females (mean = 8 SD = 10 per 10 \times 10 cross, N = 10), a statistically significant increase (p = 0.015 by Mann-Whitney test; Figure 1H). We observed a similar increase in adult progeny from crosses with infected females (mean = 14 SD = 17 per 10 \times 10 cross, N = 10) compared with uninfected females (mean = 0 SD = 0 per 10 \times 10 cross, N = 10 (p = 0.006) by Mann-Whitney test) (Figure 1I). We note that for both larval and adult counts, some hybrid crosses with infected females did not yield any progeny while others did. We interpret this bimodal mating success as indicative of how rare hybrid matings occurred in our assays—i.e., mating often did not occur, and there were likely unmated females even in the 10 \times 10 crosses producing progeny. As expected for crosses between *D. melanogaster* females and *D. simulans* males,⁶² all progeny recovered from hybrid crosses were female and sterile.

This pattern of increased progeny from infected females was also observed when *D. melanogaster* females were crossed to infected *D. simulans* males for both larvae (infected females: mean = 8 SD = 11 per 10 \times 10 cross, N = 10; uninfected females: mean = 0 SD = 0 per 10 \times 10 cross, N = 10; p = 5.9×10^{-3} by Mann-Whitney test) (Figure 1H) and adults (infected: mean = 14 SD = 17 per 10 \times 10 cross, N = 10; uninfected: mean = 18 SD = 15 per 10 \times 10 cross, N = 10; p = 7.5×10^{-4} by Mann-Whitney test; Figure 1I).

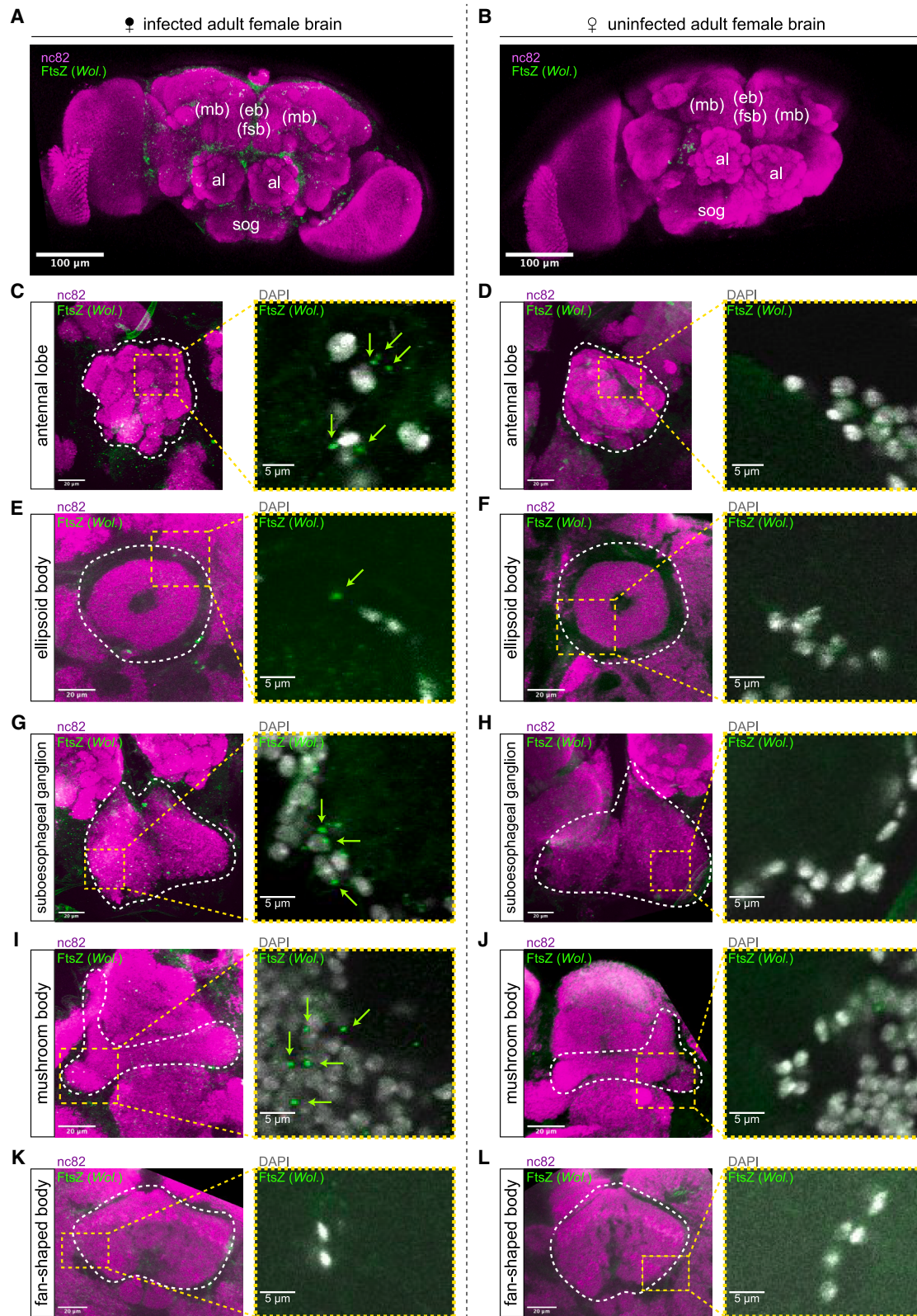
Given that we observed almost no progeny produced from uninfected females in hybrid crosses, the production of progeny from infected females suggests that *Wolbachia* infection is affecting a binary yes-or-no mating decision. Collectively,

these data demonstrate that *Wolbachia* infection in female flies produce more progeny in both intra-species and hybrid crosses in part due to a behavioral change that increases female mating receptivity to males with whom they might otherwise be reluctant to mate. Importantly, our results detail a tangible benefit for *Wolbachia* to increase female receptivity: contributing to an increased yield of infected progeny that could promote the spread of *Wolbachia* throughout a population.

Wolbachia* colonize regions in the brain known to control behavior and sense perception in *D. melanogaster

Wolbachia exhibit species- and strain-specific localization patterns in the brain.^{18,19,63,64} In *D. melanogaster*, *wMel* localizes throughout the central nervous system,¹⁹ with high concentrations in the central brain.^{18,64} Female receptivity to mating depends on sensory perception, information processing, and decision making that are controlled by neural circuits localized in specific brain regions.^{65–71} Therefore, we were interested in determining whether *Wolbachia* localized to areas of the brain involved in sensory perception and/or mating decisions.

Initially, we fixed infected and uninfected female larval brains and stained with antibodies against the bacterial protein FtsZ, which labels *Wolbachia*^{72–74} (Figure 2A). We focused on the central brain and ventral nerve cord, regions involved in higher-order and multi-sensory integration, respectively.⁷⁵ As expected, we observed multiple cytoplasmic DAPI- and FtsZ-stained puncta corresponding to *Wolbachia* in the central brain (Figure 2B) and ventral nerve cord (Figure 2C) regions of infected brains but not in the same regions of uninfected brains (Figures 2D and 2E).



(legend on next page)

We next fixed infected and uninfected female adult brains, staining with antibodies targeting FtsZ and Bruchpilot (nc82), which marks neuropils for brain region identification.⁷⁶ As with larval brains, we observed variable background staining at low magnification with the anti-FtsZ antibody in both infected and uninfected adult brains (Figures 3A and 3B). However, at higher magnification, we routinely observed bright, discernable FtsZ puncta corresponding to *Wolbachia* present only in infected brains (Figures 3C–3L). We note that, while FtsZ staining between infected brains was consistent, the level of staining was inconstant, suggesting *Wolbachia* titer may vary between brains (Figure S2A). First, we focused on five brain regions involved in sensory perception and higher-order decision making: the antennal lobes, the ellipsoid body, the suboesophageal ganglion, the mushroom bodies, and the fan-shaped body. In the adult brain, the cell bodies of the neurons surround synaptically dense neuropil into which they project their axons.⁷⁷ *Wolbachia* primarily localize to the cell bodies of neurons as opposed to their axon tracts.¹⁸ Consistent with this, we observed FtsZ-stained *Wolbachia* puncta in the cell bodies surrounding the antennal lobes in infected flies (Figure 3C) but not in those of uninfected flies (Figure 3D). We observed a similar pattern of FtsZ-stained *Wolbachia* in cell bodies surrounding infected but not uninfected ellipsoid bodies (Figures 3E–3F), suboesophageal ganglia (Figures 3G–3H), and mushroom bodies (Figures 3I–3J). However, we were unable to consistently detect FtsZ-stained puncta in fan-shaped bodies in infected and uninfected flies (Figures 3K–3L), although some infected brains did exhibit rare striking patterns of FtsZ-stained puncta overlapping the dorsal fan-shaped body (Figure S2B).

Specific doublesex-expressing neuron clusters in female flies are directly involved in making the decision to mate^{65,68,69,78} (Figure S2C). For example, vpoEN neurons respond to courtship song and innervate doublesex-expressing vpoDN neurons that directly regulate female receptive behavior.⁶⁸ In addition, the activation of doublesex-expressing pC1, which encodes mating status, and pCd neurons are necessary for female receptivity,^{65,79} with the pC1a subtype perhaps particularly important.⁶⁶ The pC1 neurons are regulated by the steroid hormone ecdysone during neural development⁷⁸ and integrate sensory information received during courtship through connections to a number of different neurons⁶⁵ (Figure S2D). To determine if *Wolbachia* localize to neuron clusters specifically involved in female receptivity, we fixed and stained infected and uninfected brains with antibodies against both FtsZ and the DNA binding domain of doublesex and focused on doublesex-positive cell bodies in the posterior female brain (Figure S2E), the area where pC1 and pCd neurons are located.^{65,66} However, we could not reliably detect FtsZ-stained puncta near doublesex-stained cell bodies in these

regions (Figure S2E), suggesting that *Wolbachia* may be absent from specific neuron clusters involved in integrating information to control female receptivity. Nevertheless, these collective results suggest that *Wolbachia* colonize many regions of the brain involved in upstream sensory perception and downstream higher-order decision-making that are important for mating.

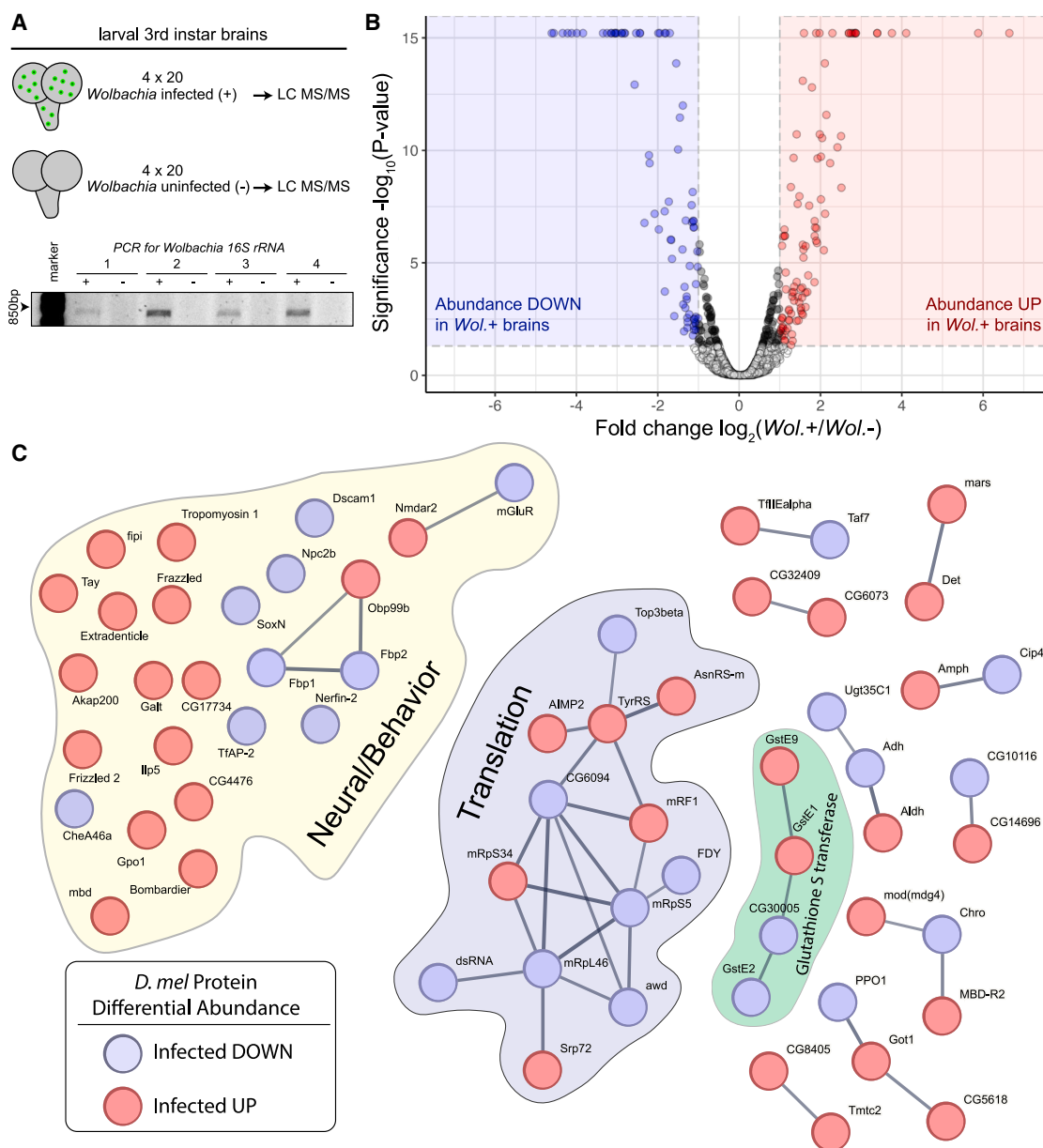
Quantitative global proteomics identified differentially abundant proteins involved in sensory perception and decision-making

Wolbachia in other tissues alter host gene expression to induce physiological change.^{32,45,50,51,80–84} However, reliable protein quantitation in these tissues has not yet been reported. Given mating involves the perception of diverse sensory information, learning, and decision making, we were particularly interested in determining the quantitative effect of *Wolbachia* on the global proteomes of infected and uninfected female brains. We hypothesized that the *Wolbachia* effect in the brain would result in measurable changes in brain proteomes and that identification of these would lead to target proteins involved in that behavior. Label-free quantitation provides an unbiased comparison of measurable proteins and provide a list of candidate target proteins for further study. We chose to analyze larval brains, because (1) the quantities needed for mass spectrometry are relatively easily attained and (2) larval brain tissue is efficiently dissected from any surrounding tissue present in heads that might otherwise confound results. In addition, much of the larval nervous tissue is remodeled to form the adult central nervous system,^{85,86} with neurodevelopmental changes occurring prior to metamorphosis affecting adult mating behavior.^{78,87,88} Therefore, we performed liquid chromatography-tandem mass spectrometry on 4 replicates each consisting of 20 *Wolbachia*-infected and 20 uninfected female larval brains (Figure 4A). We then compared the protein levels between infected and uninfected larval brains to identify differentially abundant proteins. This experimental approach was independently replicated with similar proteomic coverage and differentially abundant proteins.

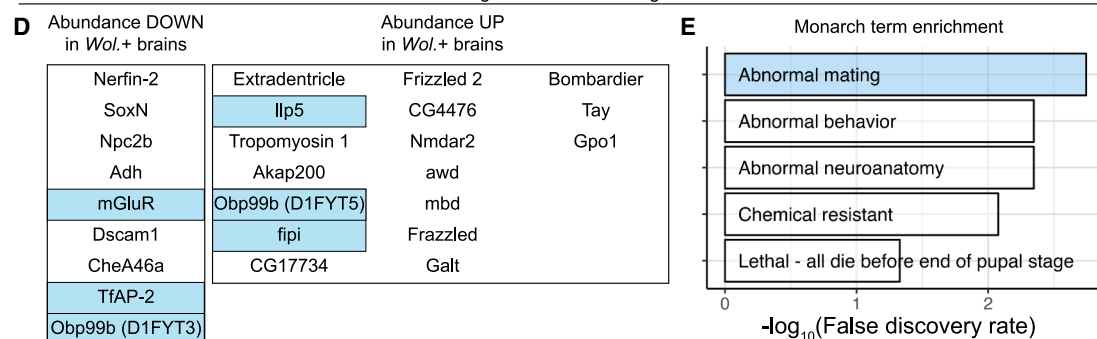
Our approach provided deep coverage of the global larval brain proteome ($n = 12,069$) of which 3,965 unique proteins could be quantified across all samples (Table S1). Of these, 177 had measurable abundance differences that met our criteria for being differentially regulated (fold change $> \pm 2$, adjusted $p < 0.05$; Figure 4B). We found that a total of 99 unique proteins were upregulated in *Wolbachia*-infected larval brains and 78 downregulated (Table S2). Analyzing potential protein-protein interactions with STRING⁸⁹ revealed a significant amount of interconnectivity (PPI enrichment $p = 1.7 \times 10^{-5}$) among the differentially expressed proteins (Figure 4C). As we were particularly interested in understanding the molecular mechanism(s)

Figure 3. *Wolbachia* colonize regions of the female adult brain involved in sensory perception and higher order decision making

(A and B) Low-magnification view of infected (A) and uninfected (B) female adult brains stained with antibodies against FtsZ (green) to label *Wolbachia* and bruchpilot/nc82 (magenta) to label neuropil. Labels correspond to the relative areas examined in (C)–(L). al, antennal lobe; eb, ellipsoid body (not visible from this view); sog, suboesophageal ganglion; mb, mushroom body (not fully visible this view); fsb, fan-shaped body (not visible from this view). Scale bars, 100 μm . (C–L) High-magnification images of the antennal lobes (C and D), ellipsoid bodies (E and F), suboesophageal ganglia (G and H), mushroom bodies (I and J), and fan-shaped bodies (K and L) of infected (C, E, G, I, and K) and uninfected (D, F, H, J, and L) flies. Dotted outlines indicate brain regions. FtsZ-stained puncta (green arrows) correspond to *Wolbachia* adjacent to DAPI-stained host cell bodies (gray). Yellow dashed boxes indicate the zoomed-in regions. Scale bars, 20 and 5 μm (for brain region and zoomed-in regions, respectively). See also Figure S2.



Long list of candidate targets



(legend on next page)

by which *Wolbachia* might increase female receptivity, we analyzed the gene ontologies of the 177 differentially regulated proteins and manually selected 25 proteins with known or predicted roles in sensory perception, learning, and/or behavior to create a candidate list of potential targets (Figure 4D). When analyzing potential interactions and biological ontologies among these candidate proteins in STRING, we found the Monarch Initiative term *Drosophila* “abnormal mating” was functionally enriched in this list. The Monarch Initiative provides ontological terms with the goal of linking phenotypes to genotypes.⁹⁰ Out of a possible 181 abnormal mating proteins, 5 (mGluR, Obp99b, fipi, TfAP-2, and Ilp5 [insulin-like peptide 5]) were present in our candidate list (Figures 4D and 4E).

We found mGluR was significantly downregulated in *Wolbachia*-infected larval brains (Figure 4D). mGluR is the only metabotropic glutamate receptor homolog present in *Drosophila* and has known roles in male courtship behavior, learning, and memory.⁹¹ We detected significantly altered levels of Obp99b in *Wolbachia*-infected larval brains (Figure 4D). Interestingly, one allele of Obp99b (D1FYT5) was more abundant in infected larval brains, while a different allele (D1FYT3 allele) was more abundant in uninfected larval brains. Obp99b is a member of the odorant binding protein family—a family of proteins important for chemoperception—and is downregulated during the post-mating response that represses female receptivity to mating.^{92,93} We found that fipi (factor of interpulse interval) was significantly upregulated in *Wolbachia*-infected larval brains (Figure 4D). Fipi expression in antennal olfactory sensory neurons is important for proper male courtship behavior.⁹⁴ We found that TfAP-2 was significantly downregulated in *Wolbachia*-infected larval brains. TfAP-2 is involved in the development of the central complex in the brain and controls octopamine production, which is necessary for a variety of behaviors including aggression and male mating behavior.^{95,96} Finally, we found that Ilp5 was significantly upregulated in *Wolbachia*-infected larval brains. Ilp5 promotes female remating.⁹⁷ Although many of these phenotypes are male-specific and governed by sexually dimorphic neural circuitry, female and male reproductive behavior can also be controlled by shared genes that have historically been studied mainly in the context of male courtship. For example, the *fruitless* gene encodes a well-characterized protein isoform responsible for male courtship behavior but also encodes an isoform that mediates female receptivity.⁹⁸ Therefore, we also considered genes with known male-specific courtship phenotypes as genes of interest.

Collectively, these results demonstrate that *Wolbachia* infection in the larval brain is quantitatively correlated with alterations in the levels of many host proteins, including a subset involved in sensory perception and mating behavior.

Neuronal depletion of mGluR in uninfected female flies phenocopies *Wolbachia* infection and promotes receptivity to mating

We next determined if the *Wolbachia*-associated upregulation and downregulation of the candidate proteins identified in our mass spectrometry results could explain the observed increased mating receptivity in infected females. We performed a genetic screen with 10 × 10 crosses between uninfected males and infected or uninfected *D. melanogaster* females bearing decreased levels of candidate proteins of interest and compared the numbers of progeny produced with those of females with wild-type levels of the proteins (Figure 5A). We reasoned that, if a target protein were upregulated in *Wolbachia*-infected larval brains (e.g., fipi, Ilp5), reducing the levels of that protein in *Wolbachia*-infected females should diminish female mating receptivity and yield lower progeny counts. Similarly, if a target protein was downregulated in *Wolbachia*-infected larval brains (e.g., TfAP-2, mGluR), decreasing that protein in uninfected females should phenocopy *Wolbachia* infection and yield increased progeny (Figure 5B). In addition, because the major allele of Obp99b detected in infected larval brains is increased upon *Wolbachia* infection, we hypothesized that, if Obp99b was a target, decreasing Obp99b in infected females should also diminish female mating. We reduced the levels of candidate proteins by reducing gene dosage using female flies heterozygous for either null mutations or chromosomal deletions overlapping the genes of interest. We created: (1) *Wolbachia*-infected females with an “Obp99b deficiency”, (2) *Wolbachia*-infected females with a “fipi deficiency”, (3) *Wolbachia*-infected females that were “Ilp5 mutant”, (4) uninfected females with an “mGluR deficiency”, and (5) uninfected females with a “TfAP-2 deficiency” (Figure 5C).

As before, crosses between *D. melanogaster* males and *Wolbachia*-infected *D. melanogaster* females produced significantly increased progeny compared with those between males and uninfected females (Figures 5D and 5E). Interestingly, infected females bearing the *Obp99b* deficiency produced significantly fewer progeny than wild-type infected females for both larval and adult counts (Figures 5D and 5E). Meanwhile, neither the *fipi* deficiency nor the *Ilp5* mutation reduced the progeny produced by *Wolbachia*-infected females (Figures 5D and 5E).

Figure 4. *Wolbachia* infection is correlated with up- and downregulation of host proteins involved in sense perception and behavior

(A) Third instar brain tissue (brain lobes and ventral nerve cords) was used for mass spectrometry. The infection status of the samples was determined by performing PCR with primers targeting *Wolbachia* on five additional brains dissected simultaneously as samples.
(B) Volcano plot of expression differences of *D. melanogaster* proteins in *Wolbachia*-infected and uninfected brains. Each dot represents one protein. Red dots are significantly upregulated in *Wolbachia*-infected brains. Blue dots are proteins significantly downregulated in *Wolbachia*-infected brain.
(C) STRING-predicted protein-protein interaction network for differentially regulated proteins in *Wolbachia*-infected brains. Red and blue dots represent proteins up- and downregulated, respectively, in *Wolbachia*-infected brains. See also Figure S3.
(D) Candidate proteins that may mediate increased female receptivity upon *Wolbachia* infection. Blue highlighted proteins were identified as belonging to the Monarch-defined “abnormal mating.”
(E) Enrichment and false discovery rates (the likelihood of a predicted enrichment being untrue) for enriched Monarch-defined phenotypes among the candidate targets depicted in (D).

Uninfected females bearing the *TfAP-2* deficiency produced significantly more larval progeny than uninfected wild-type females, but this increase was surprisingly not statistically significant for the adult counts (Figures 5D and 5E). However, uninfected females bearing the *mGluR* deficiency produced significantly increased levels of both larval and adult progeny compared with uninfected wild-type females, phenocopying the effect of *Wolbachia* infection (Figures 5D and 5E). These results suggest a potential biological meaning for the differential abundance of mGluR, Obp99b, and perhaps TfAP-2 in infected larval brains.

We next sought to determine if the observed reduction of progeny from *Obp99b*-deficient infected females and increases in progenies from *TfAP-2*- and *mGluR*-deficient uninfected females were specifically due to changes in female receptivity. We made use of hybrid crosses between *D. melanogaster* females and *D. simulans* males, which result in a binary output of progeny reflecting yes-or-no mating decisions. As before, wild-type *Wolbachia*-infected *D. melanogaster* females produced increased progeny when mated to *D. simulans* males compared with wild-type uninfected females, although this increase was only significant when counting adult progeny (Figures 5F and 5G). Infected females bearing an *Obp99b* deficiency significantly decreased progeny compared with wild-type infected females (Figures 5F and 5G). Uninfected females bearing a *TfAP-2* deficiency yielded a slight but significantly increased amount of adult, but not larval, progeny compared with wild-type uninfected females (Figures 5F and 5G). However, while this increase is statistically significant, it is only slightly higher the almost-zero baseline of progeny produced by wild-type uninfected females, indicating that alterations in the levels of TfAP-2 may have only weak effects on female receptivity. In contrast, uninfected females bearing an *mGluR* deficiency yielded a robust, significantly increased amount of progeny compared with wild-type uninfected females (Figures 5F and 5G). These results suggest that yes-or-no mating decisions contribute to the differences in progenies produced between wild-type and *mGluR*-, *Obp99b*-, and perhaps *TfAP-2*-deficient females.

These studies suggest that the reduction of mGluR in neurons contributes to *Wolbachia*-mediated alteration of mating behavior. To test this, we made use of the UAS/GAL4 system in conjunction with RNA interference (RNAi)⁹⁹ to specifically reduce levels of mGluR only in neurons. In this system, we used the pan-neuronal driver *elav-GAL4* to induce expression of RNAi targeting mGluR only in neurons ("*mGluR* RNAi")

(Figure 5C). Consistent with the *mGluR* deficiency, we observed uninfected females with decreased neuronal levels of mGluR yielded significantly increased progeny compared with uninfected wild-type females in intra-species crosses to *D. melanogaster* males (Figures 5D and 5E). Additionally, while the increased counts of larval and adult progeny from uninfected *mGluR* RNAi females crossed to *D. simulans* males was not significantly different from that of uninfected wild-type females at the specified time points (Figures 5F and 5G), we observed a significant increase in the overall number of crosses that produced progeny of any stage at any time point when mGluR was depleted (Figure 5H), reflecting increased mating success with mGluR depletion.

Collectively, these results suggest that *Wolbachia* infection increases female receptivity to mating by reducing the abundance of mGluR—and perhaps TfAP-2—and increasing the abundance Obp99b.

Detection of expressed *Wolbachia* proteins in larval brains

In addition to differentially expressed host proteins, our mass spectrometry analysis also detected 714 *Wolbachia* proteins expressed in the larval brain, of which we had abundance data for 654 (Table S3; Figure S3). The *Wolbachia* genome encodes a type IV secretion system,¹⁰⁰ which can generally be used to transfer bacterially produced proteins ("effectors") into the host cell cytoplasm. Notably, of the eight proteins that can make up the *Wolbachia* type IV secretion system, we detected seven expressed in *Wolbachia*-infected larval brains, with only VirB3 undetected (Figure 6A). Therefore, *Wolbachia* in the larval brain express the machinery capable of secreting bacterial proteins into the host cytoplasm.

Given this, we hypothesized that some of the *Wolbachia* proteins we detected in the larval brain might be bacterial effectors that could interact with host targets. Previous bioinformatic studies identified 163 potential effectors in the *Wolbachia* genome.¹⁰¹ Of these 163, we detected 117 expressed in the larval brain, 20 of which were in the top 10% of *Wolbachia* proteins detected based on abundance (Figures 6B and 6C). Additionally, prior research found that expression of 14 of these 163 *Wolbachia* genes in yeast resulted in growth defects, suggesting they might interact with eukaryotic proteins and disrupt host pathways.¹⁰¹ Notably, we detected all 14 of these candidate effectors in *Wolbachia*-infected larval brains, with WD0438 in the 10% most abundant *Wolbachia* proteins (Figures 6B and 6C).

(B) Diagram of the genetic screen. If an involved protein's abundance is increased in larval infected brains, decreasing the level of the protein in infected flies should decrease mating. If an involved protein's abundance is decreased in larval-infected brains, decreasing the level of the protein in uninfected flies should increase mating.

(C) The genotypes of female flies used in the genetic screen determining which candidate differentially abundant host proteins may be involved in *Wolbachia*-correlated increase in female receptivity.

(D and E) The numbers of larvae + pupae (D) and adults (E) collected from intra-species crosses with uninfected (white dots) and infected (black dots) *D. melanogaster* females crossed to uninfected *D. melanogaster* males. Each dot represents the progeny from one 10 × 10 cross. Data are represented as median +/– upper and lower quartiles. *p* values displayed were calculated by one-sided Mann-Whitney tests. ^{ns}*p* > 0.05, **p* < 0.05, ***p* < 0.01, ****p* < 0.001, *****p* < 0.0001.

(F and G) The numbers of larvae + pupae (F) and adults (G) collected from hybrid crosses with uninfected (white dots) and infected (black dots) *D. melanogaster* females crossed to uninfected *D. simulans* males. Each dot represents the progeny from one 10 × 10 cross. Data are represented as median +/– upper and lower quartiles. *p* values displayed were calculated by one-sided Mann-Whitney tests. ^{ns}*p* > 0.05, **p* < 0.05, *****p* < 0.0001.

(H) The percentage of hybrid crosses that produced progeny for each given female genotype and infection status. **p* < 0.05, *****p* < 0.0001 by Fisher's test.

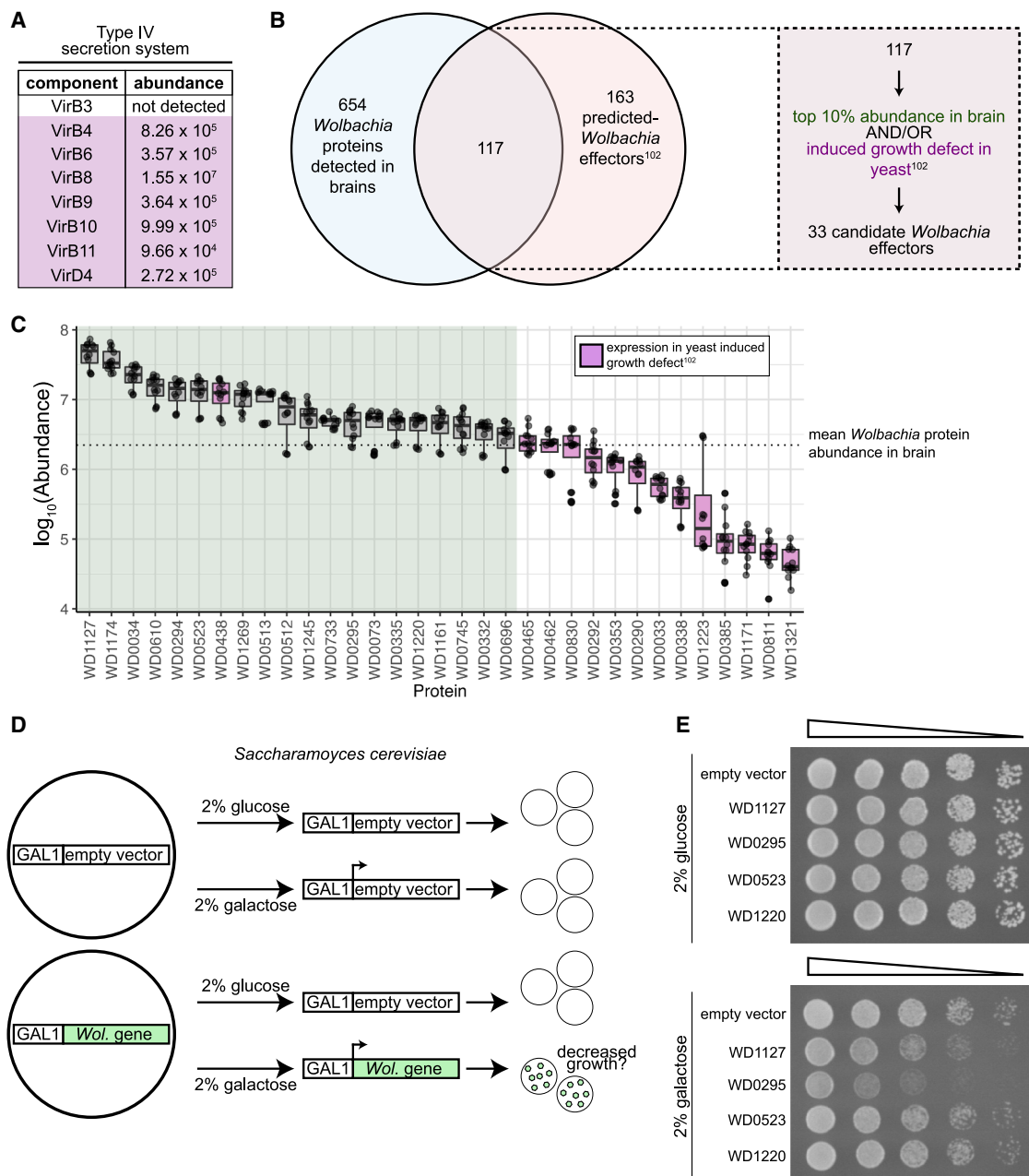


Figure 6. *Wolbachia*-produced proteins are detected in infected female brains

(A) Detected average abundances for the components of the type IV secretion system encoded by the *Wolbachia* genome. Mean *Wolbachia* protein abundance in brain = 2.22×10^6 .

(B) Diagram describing how candidate *Wolbachia* effectors were selected. WD0438 fits both selection criteria.

(C) Candidate *Wolbachia*-produced effectors detected in infected female brains. Each dot represents an individual abundance value detected for a given protein. Data are represented as median \pm upper and lower quartiles. Proteins in the green region are in the top 10% of *Wolbachia* proteins detected based on abundance. Proteins highlighted in magenta were previously identified as causing growth defects when expressed in yeast.¹⁰¹ See also Figure S4.

(D) Yeast were generated with either an empty vector or a *Wolbachia* gene of interest under control of the GAL1 promoter. Yeast were grown on either a 2% glucose control medium or 2% galactose medium to express the *Wolbachia* gene and growth was monitored with a spotting assay.

(E) Spotting assays showing a strong growth defect in yeast grown on 2% galactose expressing the *Wolbachia* proteins WD1127 or WD0295. Expression of WD0523 or WD1220 did not induce a pronounced growth defect.

We speculated that these proteins (the detected, predicted effectors either present in the top 10% of abundance or inducing a growth defect when expressed in yeast) could act as candidate *Wolbachia* effectors (Figure 6B).

We reasoned that a potential *Wolbachia*-produced effector targeting a host protein might bind that protein. Therefore, we used AlphaFold-multimer¹⁰² to predict the structures of each of the 31 candidate *Wolbachia* effectors (the 33 candidate *Wolbachia* proteins listed in Figures 6B and 6C with the exception of WD0513 and WD0385, which failed to yield results) complexing with either mGluR or Obp99b. Alongside a structure prediction, AlphaFold-multimer generates a model confidence score ranging between 0 and 1, with higher values representing increased confidence in an interface between two proteins. We used these model confidence scores as a rough guide for determining which *Wolbachia* proteins might act as effectors. Six of the 31 candidate *Wolbachia* effectors complexed with mGluR produced confidence scores significantly higher than average (Figure S4A). WD1127 produced the highest scoring complex with mGluR and was the second most abundant *Wolbachia* protein we detected in larval brains (Figure S4B). In this potential complex, WD1127 was predicted to interact with the G-protein binding domain of mGluR (Figure S4C), although the per-residue confidence was relatively low at the interface site (Figure S4C'). Additionally, 7 of the 31 candidate *Wolbachia* effectors complexed with Obp99b produced confidence scores significantly higher than average (Figure S4D). The complex between WD0295 and Obp99b was the highest scoring model for any *Wolbachia* protein with either Obp99b or mGluR (Figure S4E). WD0295 was predicted to interact with the odorant-binding domain of Obp99b (Figure S4F) with relatively high per-residue confidence at the interface site (Figure S4F').

WD1127 is predicted to contain a band 7 domain and WD0295 an ankyrin domain (Table S3). Members of the band 7/SPFH domain superfamily are involved in protein turnover,¹⁰³ and ankyrin domains are an interface for diverse protein-protein interactions.¹⁰⁴ To determine if these two potential *Wolbachia* effectors could interact with eukaryotic proteins in an *in vivo* context, we expressed WD1127 and WD0295 individually in yeast (Figure 6D) and observed a strong growth defect when either of the two *Wolbachia* proteins was expressed (Figure 6E). In contrast, neither WD0523 nor WD1220 induced notable growth defects when expressed in yeast (Figure 6E), suggesting that WD1127 and WD0295 specifically might interact with and disrupt eukaryotic pathways. We note that, while we readily observed growth defects when WD1127 and WD0295 were expressed in yeast, previous research did not,¹⁰¹ possibly due to differences in experimental design.

DISCUSSION

The parasitic manipulation hypothesis states that some parasites alter host behavior to promote their own spread.^{105,106} According to this hypothesis, the host behavioral change is mediated through the expression of parasitic genes and not an indirect host response to infection.⁸ However, the molecular mechanisms that result in host behavioral change have been challenging to address, and thus it is difficult to determine exper-

imentally if altered behavior is due to the parasite or a host response. Here, we take advantage of sophisticated molecular, genetic, and cellular approaches available in *Drosophila* to directly address this issue.

We characterized a host behavioral change in which *Wolbachia*-infected *D. melanogaster* females were more receptive to mating than uninfected females (Figure 1). Furthermore, our observation of increased mating during later time points of assays when mating has otherwise slowed, combined with previous findings in wasps that show infected females partake in increased mating with both siblings and males of any age,^{49,107} suggest that *Wolbachia* infection generally decreases female selectivity to males they would normally reject. *Wolbachia* colonized female brains, including in areas important for sensory perception and decision making (Figures 2 and 3). We identified host proteins whose levels in the larval brain changed upon *Wolbachia* infection (Figure 4). In uninfected adult female flies, the reduction of two of the proteins that were downregulated in infected larval brains, mGluR and TfAP-2, phenocopied the effect of *Wolbachia* infection by increasing receptivity to mating (Figure 5). Additionally, in infected adult female flies, the reduction of one of the proteins that was upregulated in larval infected brains, Obp99b, reduced receptivity to mating (Figure 5). We also detected components of the *Wolbachia* type IV secretion system and multiple putative bacteria-produced effectors in infected brains (Figure 6). These results suggest that, in contrast to uninfected brains (Figure 7A), the combined effect of mGluR and TfAP-2 abundance reduction and increased abundance of Obp99b in infected brains is in part responsible for the increased receptivity to mating observed in infected female flies (Figure 7B).

Previous studies on the effect of *Wolbachia* on host mating have largely focused on assortative mating and competitiveness.^{55,56,58–60,107–115} Here, we focused on the general ability of *Wolbachia* to promote host mating, which has also been observed in several different species and contexts.^{43,46,116} Our results indicate that female *Wolbachia* infection promotes *D. melanogaster* receptivity to males and that this increased receptivity may be due in part to increased virgin receptivity. This is supported by evidence of consistent hybrid mating that we would rarely observe when virgin females were uninfected. Additionally, increased receptivity may also be due in part to decreased choosiness of already-mated females, an interesting possibility given female choosiness is dependent upon pheromone responsiveness.¹¹⁷ Consistent with this, *Wolbachia* does lower female selectiveness in wasps.^{49,107} Our results build upon these studies by providing a molecular framework for the mechanisms that drive this behavioral change.

Our studies identified the glutamate receptor mGluR as a critical protein whose abundance is linked to both *Wolbachia* infection and female receptivity to mating. Glutamate signaling in *Drosophila* can be either excitatory or inhibitory and is important for proper olfaction and vision.^{118–120} Studies of the glutamatergic neuromuscular junction suggest that mGluR may act presynaptically to attenuate intense glutamatergic signaling.¹²¹ Therefore, the decreased abundance of mGluR in *Wolbachia*-infected brains may induce hyperexcitability and lead to increased receptivity to mating.

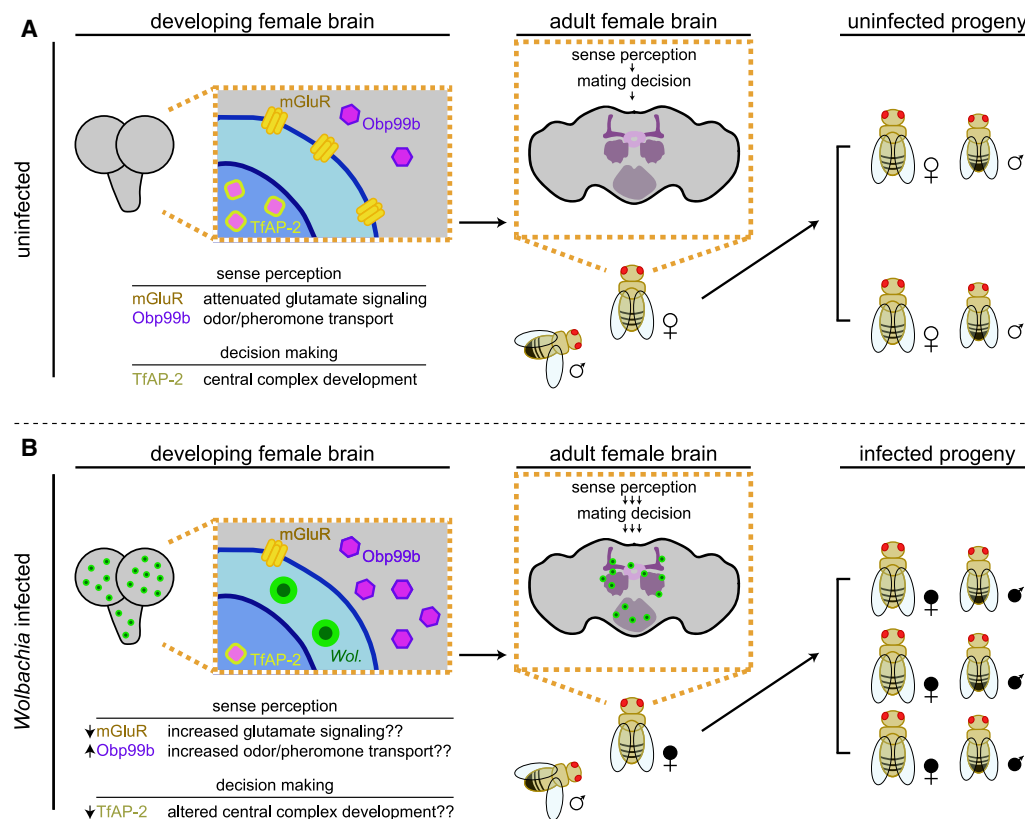


Figure 7. Model for how *Wolbachia* in the brain increases female receptivity to promote its spread

(A) In uninfected developing brains, mGluR, Obp99b, and TfAP-2 are present in wild-type levels, leading to normal sense perception and mating decisions in adult female flies. This results in the production of uninfected progeny.

(B) In *Wolbachia*-infected developing brains, mGluR and TfAP-2 levels are decreased and Obp99b levels are increased. Decreased mGluR may lead to increased excitability of glutamatergic neurons. Increased Obp99b may lead to increased odor/pheromone transport. Decreased TfAP-2 may lead to altered central complex development. In the adult brain, *Wolbachia* colonizes areas important for sense perception and decision making. Collectively, this leads to altered sense perception and mating decisions in adult females and results in increased mating and an increased amount of infected progeny.

Wolbachia localized to regions of the female adult brain known to rely on glutamatergic neurotransmission, including the antennal lobes, mushroom bodies, and ellipsoid bodies, consistent with previous results.^{18,19,64} Neurons in these regions express mGluR.^{122,123} Similarly, we detected *Wolbachia* localization in regions where mGluR is expressed in larval brains,^{122,124} which may be notable given proper mGluR expression during development is important for adult courtship behavior.^{87,88} Whether reduction of mGluR during *Wolbachia* infection occurs at the level of transcription, translation, or protein degradation is currently unknown, although we note that mGluR protein levels appear to be tightly regulated post-transcriptionally.^{87,124} However, further studies are required to determine how *Wolbachia* infection results in a reduction of mGluR protein.

Wolbachia infection also resulted in decreased abundance of TfAP-2. TfAP-2 plays a role in the development of the central complex,⁹⁶ a critical region of the brain involved in sensory perception and insect behavior.¹²⁵ Therefore, as with mGluR, *Wolbachia*-mediated reduction of TfAP-2 suggests a model in which *Wolbachia* infection in the brain disrupts neuronal pathways important for normal higher-order decision making.

Our results also fit with a growing number of -omics studies correlating *Wolbachia* infection with the altered expression of host genes involved in sense perception and reproductive behavior.^{51,80,126–129} For example, RNA-seq experiments from three *D. paulistorum* semi-species identified differentially expressed genes involved in reproduction and sense perception in *Wolbachia*-infected whole heads and abdomens.⁸⁰ Interestingly, in contrast to our findings, in these species, *Wolbachia* infection results in downregulation of Obp99b and other odorant binding proteins⁸⁰ and results in increased mate discrimination and sexual isolation.^{58,113} These discrepancies could be due to differences in the infecting *Wolbachia* strain, type of infection (obligate *wPau* vs. facultative *wMel*), and/or the host species, sex, or tissue type but suggests alteration of olfactory binding proteins may be a focal point of *Wolbachia* infection. This is particularly important given the role of certain odorant binding proteins in pheromone sensing and the role that pheromone responsiveness plays in regulating female receptivity.^{117,130}

Our studies did not establish if the actions of *Wolbachia*-produced proteins mediate the differential abundances of host proteins we detected in infected brains or if the fly regulates its own protein levels as a general response to infection. These are not

mutually exclusive possibilities. *Wolbachia* is known to produce effectors that can interact with eukaryotic gene products,¹³¹ and the potential for candidate *Wolbachia* effectors to interact with mGluR and/or Obp99b is an exciting possibility, especially given their induced growth defects when expressed in yeast.

Regardless of whether the increase in female receptivity is a host response to infection or *Wolbachia* mediated, this altered behavior ultimately benefits *Wolbachia*. Increased mating can contribute to an increased population of *Wolbachia*-infected progeny, driving the bacteria through a population, even if this difference is small (Figure S1). Given that the variant *wMel*/CS was recently replaced in natural populations by *wMel*,¹³² it would be interesting to determine if the ability to alter female receptivity differs among these two variants of *Wolbachia*. If so, this would offer a potential explanation for the preferential spread of *wMel*. In addition, increased hybrid mating between infected *D. melanogaster* females and *D. simulans* males offers an intriguing mechanism by which *Wolbachia* might promote its spread into a new species. While hybrid offspring between *D. melanogaster* and *D. simulans* are infertile, hybridization of other *Drosophila* species results in fertile offspring capable of mating with either parent.^{133,134} Interestingly, *Wolbachia* infection in *D. mauritiana* could originate from hybrid mating to infected *D. simulans*.⁴² Because hybridization is likely rare in nature,⁴¹ the fact that *Wolbachia* infection may promote this possibility would be advantageous for the bacteria.

The differentially abundant proteins we identified in *Wolbachia*-infected larval brains may be useful for aiding investigations into the mechanisms behind other behavioral changes associated with *Wolbachia* infection.⁴⁴ In addition, our global proteomic approach produced a robust *Wolbachia* proteome that will be useful for future studies of host-microbe interactions (Figure S3). For example, among the *Wolbachia* proteins we detected in larval brains, surprisingly high levels of enzymes involved in the biosynthesis of the essential amino acids methionine, lysine, and threonine were present. Coupled with the significant abundance of the type IV secretion system, the presence of these *Wolbachia*-produced enzymes suggests a possible mutualism that is mediated by increased access of the host to these essential amino acids.

Collectively, our results suggest a mechanism by which *Wolbachia* infection in the brain results in the differential abundance of host proteins, three of which—mGluR, Obp99b, and TfAP-2—stimulate increased female receptivity to mating in infected flies. Notably, the population of *Wolbachia* present in the brain mediating these changes are not transmitted to offspring. Thus, *Wolbachia* colonization of somatic central neural cells may altruistically promote transmission of *Wolbachia* in the germline.

Limitations of the study

We examined host protein changes in response to *Wolbachia* infection in the larval female brain. The relative abundance of these host proteins in adult brains is unknown. While we specifically found mGluR levels were linked to female receptivity through use of both a deficiency stock and RNAi, we examined the roles of Obp99b and TfAP-2 only with deficiency stocks, in which other genes are also deleted. Therefore, the observed effects may not be specifically linked to Obp99b and TfAP-2. In

addition, this study examined the location of *Wolbachia* in larval and adult brains through use of an anti-FtsZ antibody, which produced a large amount of background staining. The absence of FtsZ puncta corresponding to *Wolbachia* should not be interpreted as evidence of the absence of *Wolbachia* from brain regions and neurons examined. Lastly, we identified a large amount of *Wolbachia* proteins expressed in the larval brains. We used an AlphaFold-multimer approach to determine if several of these *Wolbachia* proteins might be capable of interacting with identified host targets. However, we did not validate potential interactions *in vivo*.

RESOURCE AVAILABILITY

Lead contact

Further information and requests for resources and reagents should be directed to and will be fulfilled by the lead contact, Brandt Warecki (bwarecki@ucsc.edu).

Materials availability

All unique/stable reagents generated in this study are available from the [lead contact](#) without restriction.

Data and code availability

- The top-scoring .pdb files generated are available on Zenodo: <https://doi.org/10.5281/zenodo.14110800> and are publicly available as of the date of publication.
- Proteomics data are available via ProteomeXchange: PXD058588 and are publicly available at the date of publication.
- Code and associated data used for simulations are available on Zenodo: <https://doi.org/10.5281/zenodo.14058437> and are publicly available as of the date of publication.
- Any additional information required to reanalyze the data reported in the paper is available from the [lead contact](#) upon request.

ACKNOWLEDGMENTS

We thank Benjamin Abrams (UCSC Life Sciences Microscopy Center, RRID: SCR_021135) for his technical support and assistance with microscopy experiments. We thank Kerstin Richter for her guidance on adult brain cytology. We thank Amaya Cummins for her support and assistance. We are grateful to Jessica Sandler and Kyle Tucker for technical expertise in sample preparation and mass spectrometry. Funding for these studies was provided by National Institutes of Health grant NIGMS-1R35GM139595 awarded to W.S. G.V. was supported by the NIH grant 5R25GM104552-05. The authors acknowledge resources and support from the Knowledge Enterprise Biosciences Core Facilities and the ASU-Banner Neurodegenerative Disease Research Center at Arizona State University.

AUTHOR CONTRIBUTIONS

Conceptualization, B.W., T.L.K., and W.S.; methodology, B.W., G.H., T.L.K., and W.S.; software, B.W.; validation, B.W., G.V., S.F., G.H., T.L.K., and W.S.; formal analysis, B.W. and T.L.K.; investigation, B.W., G.V., S.F., and T.L.K.; resources, G.H., T.L.K., and W.S.; data curation, B.W. and T.L.K.; writing – original draft, B.W., S.F., T.L.K., and W.S.; writing – review & editing, B.W., S.F., T.L.K., and W.S.; visualization, B.W., S.F., and T.L.K.; supervision, G.H., T.L.K., and W.S.; project administration, T.L.K. and W.S.; funding acquisition, W.S.

DECLARATION OF INTERESTS

The authors declare no competing interests.

STAR★METHODS

Detailed methods are provided in the online version of this paper and include the following:

- **KEY RESOURCES TABLE**
- **EXPERIMENTAL MODEL AND STUDY PARTICIPANT DETAILS**
 - *Drosophila* stocks
 - Yeast
- **METHOD DETAILS**
 - 10 × 10 progeny counts
 - Mating assays
 - Sample preparation for microscopy
 - Confocal imaging
 - Sample preparation for mass spectrometry
 - Liquid chromatography-tandem mass spectrometry
 - Label-free quantification (LFQ)
 - Gene ontology and PPI analyses
 - Predicting host-*Wolbachia* protein complexes with AlphaFold-multimer
 - Expression of *Wolbachia* proteins in yeast
 - Simulations
 - Experimental design
 - Figure preparation
- **QUANTIFICATION AND STATISTICAL ANALYSIS**
- **ADDITIONAL RESOURCES**

SUPPLEMENTAL INFORMATION

Supplemental information can be found online at <https://doi.org/10.1016/j.celrep.2025.115629>.

Received: December 13, 2024

Revised: March 5, 2025

Accepted: April 9, 2025

REFERENCES

1. Moore, J. (2002). *Parasites and the Behavior of Animals* (Oxford University Press).
2. Rohrscheib, C.E., and Brownlie, J.C. (2013). Microorganisms that Manipulate Complex Animal Behaviours by Affecting the Host's Nervous System. *SpringerSci. Rev.* 1, 133–140. <https://doi.org/10.1007/s40362-013-0013-8>.
3. Gowda, V., Dinesh, S., and Sharma, S. (2023). Manipulative neuromodulators: uncovering the intricacies of neurological host control. *Arch. Microbiol.* 205, 314. <https://doi.org/10.1007/s00203-023-03637-2>.
4. Boillat, M., Hammoudi, P.M., Dogga, S.K., Pagès, S., Goubran, M., Rodriguez, I., and Soldati-Favre, D. (2020). Neuroinflammation-Associated Aspecific Manipulation of Mouse Predator Fear by *Toxoplasma gondii*. *Cell Rep.* 30, 320–334.e6. <https://doi.org/10.1016/j.celrep.2019.12.019>.
5. Elya, C., Lok, T.C., Spencer, Q.E., McCausland, H., Martinez, C.C., and Eisen, M. (2018). Robust manipulation of the behavior of *Drosophila melanogaster* by a fungal pathogen in the laboratory. *Elife* 7, e34414. <https://doi.org/10.7554/eLife.34414>.
6. Vyas, A. (2015). Mechanisms of Host Behavioral Change in *Toxoplasma gondii* Rodent Association. *PLoS Pathog.* 11, e1004935. <https://doi.org/10.1371/journal.ppat.1004935>.
7. Lafferty, K.D., and Shaw, J.C. (2013). Comparing mechanisms of host manipulation across host and parasite taxa. *J. Exp. Biol.* 216, 56–66. <https://doi.org/10.1242/jeb.073668>.
8. Hunter, P. (2018). The revival of the extended phenotype: After more than 30 years, Dawkins' Extended Phenotype hypothesis is enriching evolutionary biology and inspiring potential applications. *EMBO Rep.* 19, e46477. <https://doi.org/10.15252/embr.201846477>.
9. Thomas, F., Adamo, S., and Moore, J. (2005). Parasitic manipulation: where are we and where should we go? *Behav. Processes* 68, 185–199. <https://doi.org/10.1016/j.beproc.2004.06.010>.
10. Lefevre, T., Adamo, S.A., Biron, D.G., Misse, D., Hughes, D., and Thomas, F. (2009). Invasion of the body snatchers: the diversity and evolution of manipulative strategies in host-parasite interactions. *Parasitol.* 68, 45–83. [https://doi.org/10.1016/S0065-308X\(08\)00603-9](https://doi.org/10.1016/S0065-308X(08)00603-9).
11. Cator, L.J., Pietri, J.E., Murdoch, C.C., Ohm, J.R., Lewis, E.E., Read, A. F., Luckhart, S., and Thomas, M.B. (2015). Immune response and insulin signalling alter mosquito feeding behaviour to enhance malaria transmission potential. *Sci. Rep.* 5, 11947. <https://doi.org/10.1038/srep11947>.
12. Porter, J., and Sullivan, W. (2023). The cellular lives of *Wolbachia*. *Nat. Rev. Microbiol.* 21, 750–766. <https://doi.org/10.1038/s41579-023-00918-x>.
13. Weinert, L.A., Araujo-Jnr, E.V., Ahmed, M.Z., and Welch, J.J. (2015). The incidence of bacterial endosymbionts in terrestrial arthropods. *Proc. Biol. Sci.* 282, 20150249. <https://doi.org/10.1098/rspb.2015.0249>.
14. Werren, J.H., Baldo, L., and Clark, M.E. (2008). *Wolbachia*: master manipulators of invertebrate biology. *Nat. Rev. Microbiol.* 6, 741–751. <https://doi.org/10.1038/nrmicro1969>.
15. Clark, M.E., Heath, B.D., Anderson, C.L., and Karr, T.L. (2006). Induced paternal effects mimic cytoplasmic incompatibility in *Drosophila*. *Genetics* 173, 727–734. <https://doi.org/10.1534/genetics.105.052431>.
16. Bhattacharya, T., Newton, I.L.G., and Hardy, R.W. (2017). *Wolbachia* elevates host methyltransferase expression to block an RNA virus early during infection. *PLoS Pathog.* 13, e1006427. <https://doi.org/10.1371/journal.ppat.1006427>.
17. Pietri, J.E., DeBruhl, H., and Sullivan, W. (2016). The rich somatic life of *Wolbachia*. *Microbiologyopen* 5, 923–936. <https://doi.org/10.1002/mbo3.390>.
18. Albertson, R., Tan, V., Leads, R.R., Reyes, M., Sullivan, W., and Casper-Lindley, C. (2013). Mapping *Wolbachia* distributions in the adult *Drosophila* brain. *Cell. Microbiol.* 15, 1527–1544. <https://doi.org/10.1111/cmi.12136>.
19. Strunov, A., Schneider, D.I., Albertson, R., and Miller, W.J. (2017). Restricted distribution and lateralization of mutualistic *Wolbachia* in the *Drosophila* brain. *Cell. Microbiol.* 19. <https://doi.org/10.1111/cmi.12639>.
20. Min, K.T., and Benzer, S. (1997). *Wolbachia*, normally a symbiont of *Drosophila*, can be virulent, causing degeneration and early death. *Proc. Natl. Acad. Sci. USA* 94, 10792–10796. <https://doi.org/10.1073/pnas.94.20.10792>.
21. Hedges, L.M., Brownlie, J.C., O'Neill, S.L., and Johnson, K.N. (2008). *Wolbachia* and virus protection in insects. *Science* 322, 702. <https://doi.org/10.1126/science.1162418>.
22. Cogni, R., Ding, S.D., Pimentel, A.C., Day, J.P., and Jiggins, F.M. (2021). *Wolbachia* reduces virus infection in a natural population of *Drosophila*. *Commun. Biol.* 4, 1327. <https://doi.org/10.1038/s42003-021-02838-z>.
23. Teixeira, L., Ferreira, A., and Ashburner, M. (2008). The bacterial symbiont *Wolbachia* induces resistance to RNA viral infections in *Drosophila melanogaster*. *PLoS Biol.* 6, e2. <https://doi.org/10.1371/journal.pbio.1000002>.
24. Moretti, R., Yen, P.S., Houé, V., Lampazzi, E., Desiderio, A., Failloux, A. B., and Calvitti, M. (2018). Combining *Wolbachia*-induced sterility and virus protection to fight *Aedes albopictus*-borne viruses. *PLoS Negl. Trop. Dis.* 12, e0006626. <https://doi.org/10.1371/journal.pntd.0006626>.
25. Zheng, X., Zhang, D., Li, Y., Yang, C., Wu, Y., Liang, X., Liang, Y., Pan, X., Hu, L., Sun, Q., et al. (2019). Incompatible and sterile insect techniques combined eliminate mosquitoes. *Nature* 572, 56–61. <https://doi.org/10.1038/s41586-019-1407-9>.

26. Jiggins, F.M. (2017). The spread of *Wolbachia* through mosquito populations. *PLoS Biol.* 15, e2002780. <https://doi.org/10.1371/journal.pbio.2002780>.
27. Utarini, A., Indriani, C., Ahmad, R.A., Tantowijoyo, W., Arguni, E., Ansari, M.R., Supriyati, E., Wardana, D.S., Meitika, Y., Ernesia, I., et al. (2021). Efficacy of *Wolbachia*-Infected Mosquito Deployments for the Control of Dengue. *N. Engl. J. Med.* 384, 2177–2186. <https://doi.org/10.1056/NEJMoa2030243>.
28. Kose, H., and Karr, T.L. (1995). Organization of *Wolbachia pipientis* in the *Drosophila* fertilized egg and embryo revealed by an anti-*Wolbachia* monoclonal antibody. *Mech. Dev.* 51, 275–288. [https://doi.org/10.1016/0925-4773\(95\)00372-x](https://doi.org/10.1016/0925-4773(95)00372-x).
29. Ferree, P.M., Frydman, H.M., Li, J.M., Cao, J., Wieschaus, E., and Sullivan, W. (2005). *Wolbachia* utilizes host microtubules and Dynein for anterior localization in the *Drosophila* oocyte. *PLoS Pathog.* 1, e14. <https://doi.org/10.1371/journal.ppat.0010014>.
30. Kaur, R., Shropshire, J.D., Cross, K.L., Leigh, B., Mansueto, A.J., Stewart, V., Bordenstein, S.R., and Bordenstein, S.R. (2021). Living in the endosymbiotic world of *Wolbachia*: A centennial review. *Cell Host Microbe* 29, 879–893. <https://doi.org/10.1016/j.chom.2021.03.006>.
31. Russell, S.L., Chappell, L., and Sullivan, W. (2019). A symbiont's guide to the germline. *Curr. Top. Dev. Biol.* 135, 315–351. <https://doi.org/10.1016/bs.ctdb.2019.04.007>.
32. Russell, S.L., Castillo, J.R., and Sullivan, W.T. (2023). *Wolbachia* endosymbionts manipulate the self-renewal and differentiation of germline stem cells to reinforce fertility of their fruit fly host. *PLoS Biol.* 21, e3002335. <https://doi.org/10.1371/journal.pbio.3002335>.
33. Turelli, M., Katznelson, A., and Ginsberg, P.S. (2022). Why *Wolbachia*-induced cytoplasmic incompatibility is so common. *Proc. Natl. Acad. Sci. USA* 119, e2211637119. <https://doi.org/10.1073/pnas.2211637119>.
34. Werren, J.H., Zhang, W., and Guo, L.R. (1995). Evolution and phylogeny of *Wolbachia*: reproductive parasites of arthropods. *Proc. Biol. Sci.* 261, 55–63. <https://doi.org/10.1098/rspb.1995.0117>.
35. Baldo, L., Bordenstein, S., Wernegreen, J.J., and Werren, J.H. (2006). Widespread recombination throughout *Wolbachia* genomes. *Mol. Biol. Evol.* 23, 437–449. <https://doi.org/10.1093/molbev/msj049>.
36. Russell, S.L. (2019). Transmission mode is associated with environment type and taxa across bacteria-eukaryote symbioses: a systematic review and meta-analysis. *FEMS Microbiol. Lett.* 366, fnz013. <https://doi.org/10.1093/femsle/fnz013>.
37. O'Neill, S.L., Giordano, R., Colbert, A.M., Karr, T.L., and Robertson, H.M. (1992). 16S rRNA phylogenetic analysis of the bacterial endosymbionts associated with cytoplasmic incompatibility in insects. *Proc. Natl. Acad. Sci. USA* 89, 2699–2702. <https://doi.org/10.1073/pnas.89.7.2699>.
38. Boyle, L., O'Neill, S.L., Robertson, H.M., and Karr, T.L. (1993). Interspecific and intraspecific horizontal transfer of *Wolbachia* in *Drosophila*. *Science* 260, 1796–1799. <https://doi.org/10.1126/science.8511587>.
39. Vavre, F., Fleury, F., Lepetit, D., Fouillet, P., and Boulétreau, M. (1999). Phylogenetic evidence for horizontal transmission of *Wolbachia* in host-parasitoid associations. *Mol. Biol. Evol.* 16, 1711–1723. <https://doi.org/10.1093/oxfordjournals.molbev.a026084>.
40. Schuler, H., Bertheau, C., Egan, S.P., Feder, J.L., Riegler, M., Schlick-Steiner, B.C., Steiner, F.M., Johannesen, J., Kern, P., Tuba, K., et al. (2013). Evidence for a recent horizontal transmission and spatial spread of *Wolbachia* from endemic *Rhagoletis cerasi* (Diptera: Tephritidae) to invasive *Rhagoletis cingulata* in Europe. *Mol. Ecol.* 22, 4101–4111. <https://doi.org/10.1111/mec.12362>.
41. Raychoudhury, R., Baldo, L., Oliveira, D.C.S.G., and Werren, J.H. (2009). Modes of acquisition of *Wolbachia*: horizontal transfer, hybrid introgression, and codivergence in the *Nasonia* species complex. *Evolution* 63, 165–183. <https://doi.org/10.1111/j.1558-5646.2008.00533.x>.
42. Rousset, F., and Solignac, M. (1995). Evolution of single and double *Wolbachia* symbioses during speciation in the *Drosophila simulans* complex. *Proc. Natl. Acad. Sci. USA* 92, 6389–6393. <https://doi.org/10.1073/pnas.92.14.6389>.
43. Gazla, I.N., and Carracedo, M.C. (2009). Effect of intracellular *Wolbachia* on interspecific crosses between *Drosophila melanogaster* and *Drosophila simulans*. *Genet. Mol. Res.* 8, 861–869. <https://doi.org/10.4238/vol8-3gmr595>.
44. Bi, J., and Wang, Y.F. (2020). The effect of the endosymbiont *Wolbachia* on the behavior of insect hosts. *Insect Sci.* 27, 846–858. <https://doi.org/10.1111/1744-7917.12731>.
45. Rohrscheib, C.E., Bondy, E., Josh, P., Riegler, M., Eyles, D., van Swinderen, B., Weible, M.W., 2nd, and Brownlie, J.C. (2015). *Wolbachia* Influences the Production of Octopamine and Affects *Drosophila* Male Aggression. *Appl. Environ. Microbiol.* 81, 4573–4580. <https://doi.org/10.1128/AEM.00573-15>.
46. de Crespigny, F.E.C., Pitt, T.D., and Wedell, N. (2006). Increased male mating rate in *Drosophila* is associated with *Wolbachia* infection. *J. Evol. Biol.* 19, 1964–1972. <https://doi.org/10.1111/j.1420-9101.2006.01143.x>.
47. Peng, Y., Nielsen, J.E., Cunningham, J.P., and McGraw, E.A. (2008). *Wolbachia* infection alters olfactory-cued locomotion in *Drosophila* spp. *Appl. Environ. Microbiol.* 74, 3943–3948. <https://doi.org/10.1128/AEM.02607-07>.
48. Peng, Y., and Wang, Y. (2009). Infection of *Wolbachia* may improve the olfactory response of *Drosophila*. *Sci. Bull. (Beijing)*. 54, 1369–1375. <https://doi.org/10.1007/s11434-009-0183-6>.
49. Bagheri, Z., Talebi, A.A., Asgari, S., and Mehrabadi, M. (2022). *Wolbachia* promotes successful sex with siblings in the parasitoid *Habrobracon hebetor*. *Pest Manag. Sci.* 78, 362–368. <https://doi.org/10.1002/ps.6649>.
50. Bi, J., Zheng, Y., Wang, R.F., Ai, H., Haynes, P.R., Brownlie, J.C., Yu, X. Q., and Wang, Y.F. (2019). *Wolbachia* infection may improve learning and memory capacity of *Drosophila* by altering host gene expression through microRNA. *Insect Biochem. Mol. Biol.* 106, 47–54. <https://doi.org/10.1016/j.ibmb.2018.11.007>.
51. Chen, M.-Y., Li, D., Wang, Z.-N., Xu, F.-Z., Feng, Y.-W., Yu, Q.-L., Wang, Y.-Y., Zhang, S., and Wang, Y.-F. (2024). Infection by virulent *mWolPop* *Wolbachia* improves learning and memory capacity in *Drosophila melanogaster*. *Anim. Behav.* 212, 101–112. <https://doi.org/10.1016/j.anbehav.2024.03.016>.
52. Farahani, H.K., Ashouri, A., Abroon, P., Pierre, J.S., and van Baaren, J. (2021). *Wolbachia* manipulate fitness benefits of olfactory associative learning in a parasitoid wasp. *J. Exp. Biol.* 224, jeb240549. <https://doi.org/10.1242/jeb.240549>.
53. Kishani Farahani, H., Ashouri, A., Goldansaz, S.H., Shapiro, M.S., Pierre, J.-S., and van Baaren, J. (2017). Decrease of memory retention in a parasitic wasp: an effect of host manipulation by *Wolbachia*? *Insect Sci.* 24, 569–583. <https://doi.org/10.1111/1744-7917.12348>.
54. Gazla, I., and Carracedo, M.J. (2011). *Wolbachia* induces sexual isolation in *Drosophila melanogaster* and *Drosophila simulans*. *Open J. Genet.* 1, 18–26. <https://doi.org/10.4236/ojgen.2011.12005>.
55. Koukou, K., Pavlikaki, H., Kilias, G., Werren, J.H., Bourtzis, K., and Alahiotis, S.N. (2006). Influence of antibiotic treatment and *Wolbachia* curing on sexual isolation among *Drosophila melanogaster* cage populations. *Evolution* 60, 87–96.
56. Vala, F., Egas, M., Breeuwer, J.A.J., and Sabelis, M.W. (2004). *Wolbachia* affects oviposition and mating behaviour of its spider mite host. *J. Evol. Biol.* 17, 692–700. <https://doi.org/10.1046/j.1420-9101.2003.00679.x>.
57. Bagheri, Z., Talebi, A.A., Asgari, S., and Mehrabadi, M. (2019). *Wolbachia* induce cytoplasmic incompatibility and affect mate preference in *Habrobracon hebetor* to increase the chance of its transmission to the next generation. *J. Invertebr. Pathol.* 163, 1–7. <https://doi.org/10.1016/j.jip.2019.02.005>.
58. Miller, W.J., Ehrman, L., and Schneider, D. (2010). Infectious speciation revisited: impact of symbiont-depletion on female fitness and mating

- p behavior of
- Drosophila paulistorum*
- .
- PLoS Pathog.*
- 6, e1001214.
- <https://doi.org/10.1371/journal.ppat.1001214>
- .
59. Champion de Crespigny, F.E., and Wedell, N. (2007). Mate preferences in *Drosophila* infected with *Wolbachia*? *Behav. Ecol. Sociobiol.* 61, 1229–1235.
 60. Arbuthnott, D., Levin, T.C., and Promislow, D.E.L. (2016). The impacts of *Wolbachia* and the microbiome on mate choice in *Drosophila melanogaster*. *J. Evol. Biol.* 29, 461–468. <https://doi.org/10.1111/jeb.12788>.
 61. Strunov, A., Lerch, S., Blanckenhorn, W.U., Miller, W.J., and Kapun, M. (2022). Complex effects of environment and *Wolbachia* infections on the life history of *Drosophila melanogaster* hosts. *J. Evol. Biol.* 35, 788–802. <https://doi.org/10.1111/jeb.14016>.
 62. Sturtevant, A.H. (1920). Genetic Studies on *DROSOPHILA SIMULANS*. I. Introduction. Hybrids with *DROSOPHILA MELANOGASTER*. *Genetics* 5, 488–500. <https://doi.org/10.1093/genetics/5.5.488>.
 63. Strunov, A., Kiseleva, E., and Gottlieb, Y. (2013). Spatial and temporal distribution of pathogenic *Wolbachia* strain wMelPop in *Drosophila melanogaster* central nervous system under different temperature conditions. *J. Invertebr. Pathol.* 114, 22–30. <https://doi.org/10.1016/j.jip.2013.05.001>.
 64. Albertson, R., Casper-Lindley, C., Cao, J., Tram, U., and Sullivan, W. (2009). Symmetric and asymmetric mitotic segregation patterns influence *Wolbachia* distribution in host somatic tissue. *J. Cell Sci.* 122, 4570–4583. <https://doi.org/10.1242/jcs.054981>.
 65. Zhou, C., Pan, Y., Robinett, C.C., Meissner, G.W., and Baker, B.S. (2014). Central brain neurons expressing doublesex regulate female receptivity in *Drosophila*. *Neuron* 83, 149–163. <https://doi.org/10.1016/j.neuron.2014.05.038>.
 66. Deutsch, D., Pacheco, D., Encarnacion-Rivera, L., Pereira, T., Fathy, R., Clemens, J., Girardin, C., Calhoun, A., Ireland, E., Burke, A., et al. (2020). The neural basis for a persistent internal state in *Drosophila* females. *Elife* 9, e59502. <https://doi.org/10.7554/eLife.59502>.
 67. Rideout, E.J., Dornan, A.J., Neville, M.C., Eadie, S., and Goodwin, S.F. (2010). Control of sexual differentiation and behavior by the doublesex gene in *Drosophila melanogaster*. *Nat. Neurosci.* 13, 458–466. <https://doi.org/10.1038/nn.2515>.
 68. Wang, K., Wang, F., Forknall, N., Yang, T., Patrick, C., Parekh, R., and Dickson, B.J. (2021). Neural circuit mechanisms of sexual receptivity in *Drosophila* females. *Nature* 589, 577–581. <https://doi.org/10.1038/s41586-020-2972-7>.
 69. Sakurai, A., Koganezawa, M., Yasunaga, K.I., Emoto, K., and Yamamoto, D. (2013). Select interneuron clusters determine female sexual receptivity in *Drosophila*. *Nat. Commun.* 4, 1825. <https://doi.org/10.1038/ncomms2837>.
 70. Schinaman, J.M., Giesey, R.L., Mizutani, C.M., Lukacsovich, T., and Sousa-Neves, R. (2014). The KRUPPEL-like transcription factor DATILOGRAFO is required in specific cholinergic neurons for sexual receptivity in *Drosophila* females. *PLoS Biol.* 12, e1001964. <https://doi.org/10.1371/journal.pbio.1001964>.
 71. Tompkins, L., and Hall, J.C. (1983). Identification of Brain Sites Controlling Female Receptivity in Mosaics of *DROSOPHILA MELANOGASTER*. *Genetics* 103, 179–195. <https://doi.org/10.1093/genetics/103.2.179>.
 72. Radousky, Y.A., Hague, M.T.J., Fowler, S., Paneru, E., Codina, A., Rugamas, C., Hartzog, G., Cooper, B.S., and Sullivan, W. (2023). Distinct *Wolbachia* localization patterns in oocytes of diverse host species reveal multiple strategies of maternal transmission. *Genetics* 224, iyad038. <https://doi.org/10.1093/genetics/iyad038>.
 73. Landmann, F., Bain, O., Martin, C., Uni, S., Taylor, M.J., and Sullivan, W. (2012). Both asymmetric mitotic segregation and cell-to-cell invasion are required for stable germline transmission of *Wolbachia* in filarial nematodes. *Biol. Open* 1, 536–547. <https://doi.org/10.1242/bio.2012737>.
 74. Newton, I.L.G., Savitsky, O., and Sheehan, K.B. (2015). *Wolbachia* utilize host actin for efficient maternal transmission in *Drosophila melanogaster*. *PLoS Pathog.* 11, e1004798. <https://doi.org/10.1371/journal.ppat.1004798>.
 75. Eschbach, C., and Zlatić, M. (2020). Useful road maps: studying *Drosophila* larva's central nervous system with the help of connectomics. *Curr. Opin. Neurobiol.* 65, 129–137. <https://doi.org/10.1016/j.conb.2020.09.008>.
 76. Ito, K., Shinomiya, K., Ito, M., Armstrong, J.D., Boyan, G., Hartenstein, V., Harzsch, S., Heisenberg, M., Homberg, U., Jenett, A., et al. (2014). A systematic nomenclature for the insect brain. *Neuron* 81, 755–765. <https://doi.org/10.1016/j.neuron.2013.12.017>.
 77. Spindler, S.R., and Hartenstein, V. (2010). The *Drosophila* neural lineages: a model system to study brain development and circuitry. *Dev. Genes Evol.* 220, 1–10. <https://doi.org/10.1007/s00427-010-0323-7>.
 78. Li, J., Ning, C., Liu, Y., Deng, B., Wang, B., Shi, K., Wang, R., Fang, R., and Zhou, C. (2024). The function of juvenile-adult transition axis in female sexual receptivity of *Drosophila melanogaster*. *Elife* 12. <https://doi.org/10.7554/eLife.92545>.
 79. Wang, F., Wang, K., Forknall, N., Patrick, C., Yang, T., Parekh, R., Bock, D., and Dickson, B.J. (2020). Neural circuitry linking mating and egg laying in *Drosophila* females. *Nature* 579, 101–105. <https://doi.org/10.1038/s41586-020-2055-9>.
 80. Baiao, G.C., Schneider, D.I., Miller, W.J., and Klasson, L. (2019). The effect of *Wolbachia* on gene expression in *Drosophila paulistorum* and its implications for symbiont-induced host speciation. *BMC Genom.* 20, 465. <https://doi.org/10.1186/s12864-019-5816-9>.
 81. Zhang, H.B., Cao, Z., Qiao, J.X., Zhong, Z.Q., Pan, C.C., Liu, C., Zhang, L.M., and Wang, Y.F. (2021). Metabolomics provide new insights into mechanisms of *Wolbachia*-induced paternal defects in *Drosophila melanogaster*. *PLoS Pathog.* 17, e1009859. <https://doi.org/10.1371/journal.ppat.1009859>.
 82. Gruntenko, N.E., Deryuzhenko, M.A., Andreenkova, O.V., Shishkina, O.D., Bobrovskikh, M.A., Shatskaya, N.V., and Vasiliev, G.V. (2023). *Drosophila melanogaster* Transcriptome Response to Different *Wolbachia* Strains. *Int. J. Mol. Sci.* 24, 17411. <https://doi.org/10.3390/ijms242417411>.
 83. Dou, W., Sun, B., Miao, Y., Huang, D., and Xiao, J. (2023). Single-cell transcriptome sequencing reveals *Wolbachia*-mediated modification in early stages of *Drosophila* spermatogenesis. *Proc. Biol. Sci.* 290, 20221963. <https://doi.org/10.1098/rspb.2022.1963>.
 84. Lindsey, A.R.I., Bhattacharya, T., Hardy, R.W., and Newton, I.L.G. (2021). *Wolbachia* and Virus Alter the Host Transcriptome at the Interface of Nucleotide Metabolism Pathways. *mBio* 12, e03472–20. <https://doi.org/10.1128/mBio.03472-20>.
 85. Truman, J.W., and Riddiford, L.M. (2023). *Drosophila* postembryonic nervous system development: a model for the endocrine control of development. *Genetics* 223, iyac184. <https://doi.org/10.1093/genetics/iyac184>.
 86. Diamandi, J.A., Duckhorn, J.C., Miller, K.E., Weinstock, M., Leone, S., Murphy, M.R., and Shirangi, T.R. (2024). Developmental remodeling repurposes larval neurons for sexual behaviors in adult *Drosophila*. *Curr. Biol.* 34, 1183–1193.e3. <https://doi.org/10.1016/j.cub.2024.01.065>.
 87. Stewart, R.K., Nguyen, P., Laederach, A., Volkan, P.C., Sawyer, J.K., and Fox, D.T. (2024). Orb2 enables rare-codon-enriched mRNA expression during *Drosophila* neuron differentiation. *Nat. Commun.* 15, 5270. <https://doi.org/10.1038/s41467-024-48344-8>.
 88. McBride, S.M.J., Choi, C.H., Wang, Y., Liebelt, D., Braunstein, E., Ferreiro, D., Sehgal, A., Siwicki, K.K., Dockendorff, T.C., Nguyen, H.T., et al. (2005). Pharmacological rescue of synaptic plasticity, courtship behavior, and mushroom body defects in a *Drosophila* model of fragile X syndrome. *Neuron* 45, 753–764. <https://doi.org/10.1016/j.neuron.2005.01.038>.
 89. Szklarczyk, D., Kirsch, R., Koutrouli, M., Nastou, K., Mehryary, F., Hachilif, R., Gable, A.L., Fang, T., Doncheva, N.T., Pyysalo, S., et al. (2023). The STRING database in 2023: protein-protein association networks and

- functional enrichment analyses for any sequenced genome of interest. *Nucleic Acids Res.* 51, D638–D646. <https://doi.org/10.1093/nar/gkac1000>.
90. Putman, T.E., Schaper, K., Matentzoglou, N., Rubinetti, V.P., Alquadoomi, F.S., Cox, C., Caulfield, J.H., Elsarboukh, G., Gehrke, S., Hegde, H., et al. (2024). The Monarch Initiative in 2024: an analytic platform integrating phenotypes, genes and diseases across species. *Nucleic Acids Res.* 52, D938–D949. <https://doi.org/10.1093/nar/gkad1082>.
91. Schoenfeld, B.P., Choi, R.J., Choi, C.H., Terlizzi, A.M., Hinchey, P., Kollaros, M., Ferrick, N.J., Koenigsberg, E., Ferreira, D., Leibelt, D.A., et al. (2013). The *Drosophila* DmGluRA is required for social interaction and memory. *Front. Pharmacol.* 4, 64. <https://doi.org/10.3389/fphar.2013.00064>.
92. Dalton, J.E., Kacheria, T.S., Knott, S.R., Lebo, M.S., Nishitani, A., Sanders, L.E., Stirling, E.J., Winbush, A., and Arbeitman, M.N. (2010). Dynamic, mating-induced gene expression changes in female head and brain tissues of *Drosophila melanogaster*. *BMC Genom.* 11, 541. <https://doi.org/10.1186/1471-2164-11-541>.
93. Vieira, F.G., and Rozas, J. (2011). Comparative genomics of the odorant-binding and chemosensory protein gene families across the Arthropoda: origin and evolutionary history of the chemosensory system. *Genome Biol. Evol.* 3, 476–490. <https://doi.org/10.1093/gbe/evr033>.
94. Fedotov, S.A., Bragina, J.V., Besedina, N.G., Danilenkova, L.V., Kamyshcheva, E.A., and Kamyshev, N.G. (2018). Gene CG15630 (fipi) is involved in regulation of the interpulse interval in *Drosophila* courtship song. *J. Neurogenet.* 32, 15–26. <https://doi.org/10.1080/01677063.2017.1405000>.
95. Williams, M.J., Goergen, P., Rajendran, J., Klockars, A., Kasagiannis, A., Fredriksson, R., and Schiöth, H.B. (2014). Regulation of aggression by obesity-linked genes T1AP-2 and Twz through octopamine signaling in *Drosophila*. *Genetics* 196, 349–362. <https://doi.org/10.1534/genetics.113.158402>.
96. Monge, I., Krishnamurthy, R., Sims, D., Hirth, F., Spengler, M., Kammermeier, L., Reichert, H., and Mitchell, P.J. (2001). *Drosophila* transcription factor AP-2 in proboscis, leg and brain central complex development. *Development* 128, 1239–1252. <https://doi.org/10.1242/dev.128.8.1239>.
97. Wigby, S., Slack, C., Grönke, S., Martinez, P., Calboli, F.C.F., Chapman, T., and Partridge, L. (2011). Insulin signalling regulates remating in female *Drosophila*. *Proc. Biol. Sci.* 278, 424–431. <https://doi.org/10.1098/rspb.2010.1390>.
98. Chowdhury, T., Calhoun, R.M., Bruch, K., and Moehring, A.J. (2020). The fruitless gene affects female receptivity and species isolation. *Proc. Biol. Sci.* 287, 20192765. <https://doi.org/10.1098/rspb.2019.2765>.
99. Duffy, J.B. (2002). GAL4 system in *Drosophila*: a fly geneticist's Swiss army knife. *Genesis* 34, 1–15. <https://doi.org/10.1002/gene.10150>.
100. Rances, E., Voronin, D., Tran-Van, V., and Mavingui, P. (2008). Genetic and functional characterization of the type IV secretion system in *Wolbachia*. *J. Bacteriol.* 190, 5020–5030. <https://doi.org/10.1128/JB.00377-08>.
101. Rice, D.W., Sheehan, K.B., and Newton, I.L.G. (2017). Large-Scale Identification of *Wolbachia pipientis* Effectors. *Genome Biol. Evol.* 9, 1925–1937. <https://doi.org/10.1093/gbe/evx139>.
102. Evans, R., O'Neill, M., Pritzel, A., Antropova, N., Senior, A., Green, T., Židek, A., Bates, R., Blackwell, S., Yim, J., et al. (2022). Protein complex prediction with AlphaFold-Multimer. Preprint at bioRxiv. <https://doi.org/10.1101/2021.10.04.463034>.
103. Tavernarakis, N., Driscoll, M., and Kypides, N.C. (1999). The SPFH domain: implicated in regulating targeted protein turnover in stomatins and other membrane-associated proteins. *Trends Biochem. Sci.* 24, 425–427. [https://doi.org/10.1016/S0968-0004\(99\)01467-X](https://doi.org/10.1016/S0968-0004(99)01467-X).
104. Li, J., Mahajan, A., and Tsai, M.D. (2006). Ankyrin repeat: a unique motif mediating protein-protein interactions. *Biochemistry* 45, 15168–15178. <https://doi.org/10.1021/bi062188q>.
105. Poulin, R., and Maure, F. (2015). Host Manipulation by Parasites: A Look Back Before Moving Forward. *Trends Parasitol.* 31, 563–570. <https://doi.org/10.1016/j.pt.2015.07.002>.
106. Holmes, J.C., and Bethel, W.M. (1972). Modification of intermediate host behavior by parasites. *Behavioral Aspects of Parasite Transmission*. E.U. Canning and C.A. Wright, eds. Academic Press, pp. 123–149.
107. Amini, S., Fathipour, Y., Hoffmann, A., and Mehrabadi, M. (2024). *Wolbachia* affect female mate preference and offspring fitness in a parasitoid wasp. *Pest Manag. Sci.* 80, 5432–5439. <https://doi.org/10.1002/ps.8272>.
108. Zhao, D.X., Zhang, X.F., Chen, D.S., Zhang, Y.K., and Hong, X.Y. (2013). *Wolbachia*-Host Interactions: Host Mating Patterns Affect *Wolbachia* Density Dynamics. *PLoS One* 8, e66373. <https://doi.org/10.1371/journal.pone.0066373>.
109. Jiggins, F.M., Randerson, J.P., Hurst, G.D.D., and Majerus, M.E.N. (2002). How can sex ratio distorters reach extreme prevalences? Male-killing *Wolbachia* are not suppressed and have near-perfect vertical transmission efficiency in *Acraea encedon*. *Evolution* 56, 2290–2295. <https://doi.org/10.1111/j.0014-3820.2002.tb00152.x>.
110. Sullivan, J., and Jaenike, J. (2006). Male-killing *Wolbachia* and male mate choice: a test with *Drosophila innubila*. *Evol. Ecol. Res.* 8, 91–102.
111. Panteleev, D.I., Goriacheva, I.I., Andrianov, B.V., Reznik, N.L., Lazebny, O.E., and Kulikov, A.M. (2007). [The endosymbiotic bacterium *Wolbachia* enhances the nonspecific resistance to insect pathogens and alters behavior of *Drosophila melanogaster*]. *Genetika* 43, 1277–1280.
112. Markov, A.V., Lazebny, O.E., Goryacheva, I.I., Antipin, M.I., and Kulikov, A.M. (2009). Symbiotic bacteria affect mating choice in *Drosophila melanogaster*. *Anim. Behav.* 77, 1011–1017. <https://doi.org/10.1016/j.anbehav.2009.01.011>.
113. Schneider, D.I., Ehrman, L., Engl, T., Kaltenpoth, M., Hua-Van, A., Le Rouzic, A., and Miller, W.J. (2019). Symbiont-Driven Male Mating Success in the Neotropical *Drosophila paulistorum* Superspecies. *Behav. Genet.* 49, 83–98. <https://doi.org/10.1007/s10519-018-9937-8>.
114. Fortin, M., Debenest, C., Souty-Grosset, C., and Richard, F.J. (2018). Males prefer virgin females, even if parasitized, in the terrestrial isopod *Armadillidium vulgare*. *Ecol. Evol.* 8, 3341–3353. <https://doi.org/10.1002/ece3.3858>.
115. Tourani, A.H., Katlav, A., Cook, J.M., and Riegler, M. (2024). Mating receptivity mediated by endosymbiont interactions in a haplodiploid thrips species. *Proc. Biol. Sci.* 291, 20241564. <https://doi.org/10.1098/rspb.2024.1564>.
116. Osorio, J., Villa-Arias, S., Camargo, C., Ramírez-Sánchez, L.F., Barrientos, L.M., Bedoya, C., Rúa-Urbe, G., Dorus, S., Alfonso-Parra, C., and Avila, F.W. (2023). wMel *Wolbachia* alters female post-mating behaviors and physiology in the dengue vector mosquito *Aedes aegypti*. *Commun. Biol.* 6, 865. <https://doi.org/10.1038/s42003-023-05180-8>.
117. Kohlmeier, P., Zhang, Y., Gorter, J.A., Su, C.Y., and Billeter, J.C. (2021). Mating increases *Drosophila melanogaster* females' choosiness by reducing olfactory sensitivity to a male pheromone. *Nat. Ecol. Evol.* 5, 1165–1173. <https://doi.org/10.1038/s41559-021-01482-4>.
118. Liu, W.W., and Wilson, R.I. (2013). Glutamate is an inhibitory neurotransmitter in the *Drosophila* olfactory system. *Proc. Natl. Acad. Sci. USA* 110, 10294–10299. <https://doi.org/10.1073/pnas.1220560110>.
119. Mauss, A.S., Pankova, K., Arenz, A., Nern, A., Rubin, G.M., and Borst, A. (2015). Neural Circuit to Integrate Opposing Motions in the Visual Field. *Cell* 162, 351–362. <https://doi.org/10.1016/j.cell.2015.06.035>.
120. Richter, F.G., Fendl, S., Haag, J., Drews, M.S., and Borst, A. (2018). Glutamate Signaling in the Fly Visual System. *iScience* 7, 85–95. <https://doi.org/10.1016/j.isci.2018.08.019>.
121. Bogdanik, L., Mohrmann, R., Ramaekers, A., Bockaert, J., Grau, Y., Brodie, K., and Parmentier, M.L. (2004). The *Drosophila* metabotropic glutamate receptor DmGluRA regulates activity-dependent synaptic

- facilitation and fine synaptic morphology. *J. Neurosci.* 24, 9105–9116. <https://doi.org/10.1523/JNEUROSCI.2724-04.2004>.
122. Ramaekers, A., Parmentier, M.L., Lasnier, C., Bockart, J., and Grau, Y. (2001). Distribution of metabotropic glutamate receptor DmGlu-A in *Drosophila melanogaster* central nervous system. *J. Comp. Neurol.* 438, 213–225. <https://doi.org/10.1002/cne.1310>.
123. Kahsai, L., Carlsson, M.A., Winther, A.M.E., and Nässel, D.R. (2012). Distribution of metabotropic receptors of serotonin, dopamine, GABA, glutamate, and short neuropeptide F in the central complex of *Drosophila*. *Neuroscience* 208, 11–26. <https://doi.org/10.1016/j.neuroscience.2012.02.007>.
124. Pan, L., Woodruff, E., 3rd, Liang, P., and Broadie, K. (2008). Mechanistic relationships between *Drosophila* fragile X mental retardation protein and metabotropic glutamate receptor A signaling. *Mol. Cell. Neurosci.* 37, 747–760. <https://doi.org/10.1016/j.mcn.2008.01.003>.
125. Wolff, T., and Rubin, G.M. (2018). Neuroarchitecture of the *Drosophila* central complex: A catalog of nodulus and asymmetrical body neurons and a revision of the protocerebral bridge catalog. *J. Comp. Neurol.* 526, 2585–2611. <https://doi.org/10.1002/cne.24512>.
126. Detcharoen, M., Schilling, M.P., Arthofer, W., Schlick-Steiner, B.C., and Steiner, F.M. (2021). Differential gene expression in *Drosophila melanogaster* and *D. nigrosparsa* infected with the same *Wolbachia* strain. *Sci. Rep.* 11, 11336. <https://doi.org/10.1038/s41598-021-90857-5>.
127. Wimalasiri-Yapa, B.M.C.R., Huang, B., Ross, P.A., Hoffmann, A.A., Ritchie, S.A., Frentiu, F.D., Warrilow, D., and van den Hurk, A.F. (2023). Differences in gene expression in field populations of *Wolbachia*-infected *Aedes aegypti* mosquitoes with varying release histories in northern Australia. *PLoS Negl. Trop. Dis.* 17, e0011222. <https://doi.org/10.1371/journal.pntd.0011222>.
128. Frantz, S.I., Small, C.M., Cresko, W.A., and Singh, N.D. (2023). Ovarian transcriptional response to *Wolbachia* infection in *D. melanogaster* in the context of between-genotype variation in gene expression. *G3 (Bethesda)* 13, jkad047. <https://doi.org/10.1093/g3journal/jkad047>.
129. Chen, M.-Y., Wang, Z.-N., Fengzhen, X., Feng, Y.-W., Yu, Q.-L., and Wang, Y.-F. (2021). Effect of *Wolbachia* infection on the head transcriptome of *Drosophila melanogaster*. *J. Plant Protect.* 48, 1422–1428. <https://doi.org/10.13802/j.cnki.zwbhxb.2021.2021897>.
130. Xu, P., Atkinson, R., Jones, D.N.M., and Smith, D.P. (2005). *Drosophila* OBP LUSH is required for activity of pheromone-sensitive neurons. *Neuron* 45, 193–200. <https://doi.org/10.1016/j.neuron.2004.12.031>.
131. Ote, M., Ueyama, M., and Yamamoto, D. (2016). *Wolbachia* Protein TomO Targets nanos mRNA and Restores Germ Stem Cells in *Drosophila* Sex-lethal Mutants. *Curr. Biol.* 26, 2223–2232. <https://doi.org/10.1016/j.cub.2016.06.054>.
132. Strunov, A., Kirchner, S., Schindelar, J., Kruckenhauser, L., Haring, E., and Kapun, M. (2023). Historic Museum Samples Provide Evidence for a Recent Replacement of *Wolbachia* Types in European *Drosophila melanogaster*. *Mol. Biol. Evol.* 40, msad258. <https://doi.org/10.1093/molbev/msad258>.
133. Barbash, D.A. (2010). Ninety years of *Drosophila melanogaster* hybrids. *Genetics* 186, 1–8. <https://doi.org/10.1534/genetics.110.121459>.
134. Lachaise, D., David, J.R., Lemeunier, F., Tsacas, L., and Ashburner, M. (1986). The Reproductive Relationships of *Drosophila* Sechellia with *D. Mauritiana*, *D. Simulans*, and *D. Melanogaster* from the Afrotropical Region. *Evolution* 40, 262–271. <https://doi.org/10.1111/j.1558-5646.1986.tb00468.x>.
135. Wu, M., Sun, L.V., Vamathevan, J., Riegler, M., Deboy, R., Brownlie, J.C., McGraw, E.A., Martin, W., Esser, C., Ahmadinejad, N., et al. (2004). Phylogenomics of the reproductive parasite *Wolbachia pipientis* wMel: a streamlined genome overrun by mobile genetic elements. *PLoS Biol.* 2, E69. <https://doi.org/10.1371/journal.pbio.0020069>.
136. Casper-Lindley, C., Kimura, S., Saxton, D.S., Essaw, Y., Simpson, I., Tan, V., and Sullivan, W. (2011). Rapid fluorescence-based screening for *Wolbachia* endosymbionts in *Drosophila* germ line and somatic tissues. *Appl. Environ. Microbiol.* 77, 4788–4794. <https://doi.org/10.1128/AEM.00215-11>.
137. Serbus, L.R., White, P.M., Silva, J.P., Rabe, A., Teixeira, L., Albertson, R., and Sullivan, W. (2015). The impact of host diet on *Wolbachia* titer in *Drosophila*. *PLoS Pathog.* 11, e1004777. <https://doi.org/10.1371/journal.ppat.1004777>.
138. Simoes, P.M., Mialdea, G., Reiss, D., Sagot, M.F., and Charlat, S. (2011). *Wolbachia* detection: an assessment of standard PCR protocols. *Mol. Ecol. Resour.* 11, 567–572. <https://doi.org/10.1111/j.1755-0998.2010.02955.x>.
139. Wickham, H. (2016). *ggplot2: Elegant Graphics for Data Analysis* (Springer-Verlag).
140. Cianfrocco, M.A., Wong-Barnum, M., Youn, C., Wagner, R., and Leschziner, A. (2017). COSMIC2: A Science Gateway for Cryo-Electron Microscopy Structure Determination. Practice and Experience in Advanced Research Computing 2017: Sustainability, Success and Impact. Association for Computing Machinery, 1–5.
141. Sullivan, W., Ashburner, A., and Hawley, R.S. (2000). *Drosophila Protocols* (Cold Spring Harbor Laboratory Press).
142. Lin, D.M., and Goodman, C.S. (1994). Ectopic and increased expression of Fasciclin II alters motoneuron growth cone guidance. *Neuron* 13, 507–523. [https://doi.org/10.1016/0896-6273\(94\)90022-1](https://doi.org/10.1016/0896-6273(94)90022-1).
143. Rose, M.D., Winston, F., and Hieter, P. (1990). *Methods in Yeast Genetics: A Laboratory Course Manual* (Cold Spring Harbor Laboratory Press).
144. Perez-Riverol, Y., Bai, J., Bandla, C., García-Seisdedos, D., Hewapathirana, S., Kamatchinathan, S., Kundu, D.J., Prakash, A., Frericks-Zipper, A., Eisenacher, M., et al. (2022). The PRIDE database resources in 2022: a hub for mass spectrometry-based proteomics evidences. *Nucleic Acids Res.* 50, D543–D552. <https://doi.org/10.1093/nar/gkab1038>.
145. Deutsch, E.W., Bandeira, N., Perez-Riverol, Y., Sharma, V., Carver, J.J., Mendoza, L., Kundu, D.J., Wang, S., Bandla, C., Kamatchinathan, S., et al. (2023). The ProteomeXchange consortium at 10 years: 2023 update. *Nucleic Acids Res.* 51, D1539–D1548. <https://doi.org/10.1093/nar/gkac1040>.
146. Sheehan, K.B., Martin, M., Lesser, C.F., Isberg, R.R., and Newton, I.L.G. (2016). Identification and Characterization of a Candidate *Wolbachia pipientis* Type IV Effector That Interacts with the Actin Cytoskeleton. *mBio* 7, e00622-16. <https://doi.org/10.1128/mBio.00622-16>.

STAR★METHODS

KEY RESOURCES TABLE

REAGENT or RESOURCE	SOURCE	IDENTIFIER
Antibodies		
Anti-rabbit-488 (Goat)	ThermoFisher Scientific	Cat#A-11008; RRID:AB_143165
Anti-mouse-568 (Goat)	Invitrogen	Cat#A-11004; RRID:AB_2534072
Anti-nc82 (bruchpilot) (Mouse)	Developmental Studies Hybridoma Bank	Cat#AB_2314866; RRID:AB_2314866
Anti-DoublesexDBD (Mouse)	Developmental Studies Hybridoma Bank	Cat#AB_2617197; RRID:AB_2617197
Anti-FtsZ (Rabbit)	Lab of Irene Newton (Newton et al. ⁷⁴)	RRID:AB_3676370
Bacterial and virus strains		
<i>Wolbachia</i> (wMel)	Wu et al. ¹³⁵	https://www.ncbi.nlm.nih.gov/nucleotide/NC_002978
10-beta competent <i>E. coli</i> (High efficiency)	New England Biolabs	Cat#C30191
Chemicals, peptides, and recombinant proteins		
Sequencing Grade Modified Trypsin	Promega	Cat#V5111
Phosphoric Acid	Millipore Sigma	Cat#345245
Iodoacetamide (IAA)	ThermoFisher Scientific	Cat#A39271
Sodium dodecyl sulfate (SDS)	Fisher Scientific	Cat#NC0843525
TEAB	ThermoFisher Scientific	Cat#PI90114
Dithiothreitol (DTT)	Millipore Sigma	Cat#43816-10
Formic Acid	ThermoFisher Scientific	Cat#PI28905
Acetonitrile	Fisher Scientific	Cat#A955-4
Critical commercial assays		
NEBridge Golden Gate Assembly Kit (BSal-HF-V2)	New England Biolabs	Cat#E1601L
Nucleospin Plasmid EasyPure	Takara Bio	Cat#740727.25
EZQ Protein Quantitation Kit	ThermoFisher Scientific	Cat#R33200
Pierce BCA Protein Assay Kit	ThermoFisher Scientific	Cat#23225
S-Trap Micro Column	Profi	Cat#C02-micro-80
Deposited data		
<i>Wolbachia</i> spread simulations	Zenodo	Zenodo: https://doi.org/10.5281/zenodo.14058437
Top-scoring predicted protein complexes between candidate <i>Wolbachia</i> effectors and mGluR or Obp99b	Zenodo	Zenodo: https://doi.org/10.5281/zenodo.14110800
Proteomics datasets for <i>Wolbachia</i> -infected and uninfected third instar female brains	PRIDE (ProteomeXchange)	ProteomeXchange: PXD058588
Experimental models: Organisms/strains		
<i>D. melanogaster</i> : wild-type uninfected: Oregon_R-derived	Lab of William Sullivan (Albertson et al. ¹⁸ ; Ferree et al. ²⁹)	N/A
<i>D. melanogaster</i> : wild-type, <i>Wolbachia</i> (wMel)-infected: Oregon_R-derived	Lab of William Sullivan (Albertson et al. ¹⁸ ; Ferree et al. ²⁹)	N/A
<i>D. simulans</i> : uninfected: w-	Lab of William Sullivan (Casper-Lindley et al. ¹³⁶)	N/A
<i>D. simulans</i> : <i>Wolbachia</i> (wRi)-infected: w-	Lab of William Sullivan (Serbus et al. ¹³⁷)	N/A

(Continued on next page)

Continued

REAGENT or RESOURCE	SOURCE	IDENTIFIER
<i>D. melanogaster</i> : <i>Obp99b</i> deficiency (<i>Wolbachia</i> -infected): w[1118]; Df(3R)BSC547/TM6C, Sb[1]	Bloomington <i>Drosophila</i> Stock Center	RRID:BDSC_25075
<i>D. melanogaster</i> : <i>flpi</i> deficiency (uninfected): w[1118]; Df(2L)ED250, P{w[+mW.Scer ^{FRT} .hs3]=3'.RS5+3.3'} ED250/ln(2L)Cy[L]t[R] ln(2R)Cy, Duox[Cy] amos[Roi-1]	Bloomington <i>Drosophila</i> Stock Center	RRID:BDSC_9270
<i>D. melanogaster</i> : <i>flpi</i> deficiency (<i>Wolbachia</i> -infected): w[1118]/+; Df(2L)ED250, P{w[+mW.Scer ^{FRT} .hs3]=3'.RS5+3.3'}ED250/+	This paper	N/A
<i>D. melanogaster</i> : <i>llp5</i> mutant (uninfected): w[1118]; Tl{w[+mW.hs]=Tl}llp5[1]	Bloomington <i>Drosophila</i> Stock Center	RRID:BDSC_30884
<i>D. melanogaster</i> : <i>llp5</i> mutant (<i>Wolbachia</i> -infected): w[1118]/+; Tl{w[+mW.hs]=Tl}llp5[1]/+	This paper	N/A
<i>D. melanogaster</i> : <i>TfAP-2</i> deficiency (<i>Wolbachia</i> -infected): w[1118]; Df(3L)ED4978, P{w[+mW.Scer ^{FRT} .hs3]=3'.RS5+3.3'}ED4978/TM6C, cu[1] Sb[1]	Bloomington <i>Drosophila</i> Stock Center	RRID:BDSC_8101
<i>D. melanogaster</i> : <i>TfAP-2</i> deficiency (uninfected): w[1118]/+; Df(3L)ED4978, P{w[+mW.Scer ^{FRT} .hs3]=3'.RS5+3.3'}ED4978/+	This paper	N/A
<i>D. melanogaster</i> : <i>mGluR</i> deficiency (<i>Wolbachia</i> -infected): y[1] w[67c23]; Df(4)8-M318, P{w[+mW.hs] = hsp26-pt-T}8-M318/ln(4)ci[D], ci[D] pan[ciD]	Bloomington <i>Drosophila</i> Stock Center	RRID:BDSC_84132
<i>D. melanogaster</i> : <i>mGluR</i> deficiency (uninfected): y[1] w[67c23]/+; Df(4)8-M318, P{w[+mW.hs] = hsp26-pt-T}8-M318/+	This paper	N/A
<i>D. melanogaster</i> : <i>mGluR</i> RNAi: y[1] v[1]; P{y[+t7.7] v[+t1.8] = TriP.JF01958}attP2	Bloomington <i>Drosophila</i> Stock Center	RRID:BDSC_25938
<i>D. melanogaster</i> : elav-Gal4: Elav-Gal4	Bloomington <i>Drosophila</i> Stock Center	RRID:BDSC_458
<i>D. melanogaster</i> : <i>mGluR</i> RNAi (uninfected): Elav-Gal4/y[1] v[1]; H2Av-RFP/+; P{y[+t7.7] v[+t1.8] = TriP.JF01958}attP2	This paper	N/A
<i>S. cerevisiae</i> : GHY2311: <i>MATa his3Δ1 lys2Δ0 leu2Δ0 ura3Δ0 bar1Δ::NATMX</i>	Lab of Grant Hartzog	N/A
Oligonucleotides		
<i>Wolbachia</i> 16S rRNA forward primer: ATACGGAGAGGGCTAGCGTT	Integrated DNA Technologies; Simões et al. ¹³⁸	N/A
<i>Wolbachia</i> 16S rRNA reverse primer: CTCATRYACTCGAGTTGCWGAGT	Integrated DNA Technologies; Simões et al. ¹³⁸	N/A
Codon-optimized WD0295: TTATTCGTCGGGTCTCT AATGAAAGACTATCACCAATTGCGTCCACTTCACCT TCGTCACCAAGTATTCTATCACGAAGGAAGCCAAGT GCGACTTATCGTACGATAACGCTTCCGACAATTCA TCTCAGTCTGATGAGATTGGGTATAACAAGATCGG GGCAACAAGTGGCGCAAGCAAGCCCTCATCTTGG ATCGACGCGGTAAAGGCGCTTTTCAGTTTATTAG CTCTCCATTGAGGGCAGCTCTACCATCGTTTTCTG AAAACTCTAGCTCCAGATCCGGAACAGCTGGATCA TCGTGAATCATTGATACAGTCAGGAACCCCTAAC ATTCAGTACACTTCACAATTCTCAAGAGAGGTATGT GCTAGTAACAATGCTTCTTTGATGTTCTTCTATTGC AGGCGTTCTTAGACAAGAAGTGCCCCCTACCCAAA	Twist Bioscience	N/A

(Continued on next page)

Continued

REAGENT or RESOURCE	SOURCE	IDENTIFIER
TTTTCAGATGTAACCCAGTTAAGGCTTTATTTTATACATCGGACATCATAAAACGTGTTCAAAGAGGTTTATGAGAAGCAAGCCGAGTCAAAGGGTGGCATCAAATGCATAGATTGGATATTAACCTCGAGAAGTTGTTGAGAAGATCAACGAGAAGATAAGATCGGGAGAATTCAACGAAATTTCAGGTATCTTGAAGTCATATGCAGAAGAGGCTCTACCGGCGAGGGAGCCCGAGATCCTGGTAGATTGTCCCCTAAGAAGTTTGACAAGTTTCATGGCAGAGTTTAAACAGACGTATAGACCCCGTCATTAAACCAGCTGATGCAGCAGATGTTAAGTAGATTGGAAGTGTCGACGTAAAGGAGCAGCAGATATCTTTGGAACCTAAGCTTATCTGAATAACACGTCAGTTCAATGCCATTTAACACAAGCGCGTGGCCAGGGTAAGGTTCTAATTCCTTG AAGAGCTTAGAGACCGGTACTAGTTCCT		
Codon-optimized WD1127: TTATTCGTCGGGTCTCTAATGTTACAGGGAAGAACGAAAAGTCAACCTCTATATTGGCAAAAGTGGGTAAACGCTGCATCAGGTGTGGGATCTTTCCTTGGAAGGGCGCTCAAAGTACTAGTCAAAGGCGCTGTATACCCTATCTGGCCAAAGAACTGGTTCAAGTCCTGGGATGAAATGCGTCAACGACATAAAGAATGGCGGAAGGAGCATCATAGGAAACCCATTAGAGGAGTACGACCCTACCATAGAGACTACCCAGGCGTCTGAGGATTTAGGAGTCCAGATCATGGAACAGAAGAAGGGAACCGGTAAGGTGACATTCTTAGCGTCCAGAACTTTAACCGGCGACATCCCTACTTGACACCAGAGAGAC TAGGTGAGATCAAGCAGAACCTGCCTAATGTGACCATCTTTAAAGAAGAGAATAAGATAGTTATAGAGGTTGACGTCAAGAAGATCATAGAGACATAAAGTATAAAGGGAAATCGCCAGAGGAGATCAAGAAGTTAGCAATCGAGGAGATAAAGCAAAAGGTTGATGGCAACCTTAAGGACCTGGCCAAGATCACAGGTGGCGAATTCAAAGTACACACAGACCTTAACTTCTGTACGGAATAGCAGAAAAGCTATACAAGGAGTATGACAACCAGAGCAGTCATCCGACAAGGTGGTAAAATCCGATGTAGGTCAGCCTTCTGAGACAATAGCTTCA GGAGAAAAGAAATGGGCGCAGGAAGCTATAAAGGCTGGTAAAAGTCAGAGTTGCGGTATGCA GAAGTGAAGAGCTTAGAGACCGGTACTAGTTCCT	Twist Bioscience	N/A
Codon-optimized WD0523: TTATTCGTCGGGTCTCTAATGTTTAATAAAGTTCGGTGTGAAGACCGTTCTAATAGACTATAACAAGATCATTAACTCTAAAGGAGATACAGGAGAAGTCCTTGATATTCGCCAAGCAGGACGAGACTTTGGCTAAGAAGTTGACTTTAGATAGGATCAAAGTAGAGGTTGCTAAGTTCGTTAAAGAGCACAAAGATAACAGAATTTTCATCCCCGATAATTTACACTCAGCCCCGACCCCTTGCAAGGCAGCTGGTCACAGAGGCAATAGTTAAGATAGTCGACGACAACCCCGCAATTCACCTTGTGGGAATATGCGAGGGCATAATGAACGCTAAGGGAATAGAAGTAGTCTCGGTGGTATCAGATGAGGAGAAAGGAGAAGTCACCTTGAAATCGGCTCCCAA TCCACAGAAAGAGGATTTGCCTTTGCAGCAGATAAAGATCGTACCTAACAGTCGTTTAGCTGAGGTAGTAGCTAAGTTCCTTATCCCCAACGAGACGGTTGGTTCAGGCACATATTTCCCGACGCG	Twist Bioscience	N/A

(Continued on next page)

Continued

REAGENT or RESOURCE	SOURCE	IDENTIFIER
CACAGCGGCGCGCTCTCCAATACACCAGAGA ATCGTAGGAAATTAGAGTCCTTGGGATACAA GTCGCTGCATTTCAGTTCCGAGGGCGTCATAG AGGCCATCGAGGACAAACACGGCAACGTTCA TTTTCAGAGCCACCCAGAAGCGTTGGTGGTCA AATCTGACAAGAACCTATACCTTTCAAATCACA AAGAGAGACAGGTTTCCACGCTTGAGCTATC GCTATCATGAATGACTTCTGTACCGTGCTTG AAGAGCTTAGAGACCGGTACTAGTTCCT		
Codon-optimized WD1220: TTATTCGTGCGGTCTCTA ATGAGCATTTGTTTCTGTAATCGAAGGCTTGATGT ACAAGTACATAACGATACAGAACATCACAATGAAGA AGTACATATTCTTATTAGCGCTTGCCCAATGCTTG TGGGCATCACATTATACTTGCTGAGAAATATCGACA ATACGAAACAGAGTATTACAGCTGGAGATAAATTCT ACGAGGTATTGTTCTAAAGAAAGACAACAAGCCA CTACTTGAAGAGATCGACTCCAATTGGGAATATTT GGCTAACTTCGAGAGAGCATTTAACCACATCTCC GATAGTATGCCTACAGACACTGCTTCCATTACAA TGACCTTGCCGACGATAAAGACGCTCCGAACGTA TTAAGGGAGCTTGCTCAGTACCTGGAAGTGATGT CACTATTACACAGCAACGGAGAGAAGATTAAACA GGATAAGATTGATAATTTGGAGTCCAGCACAGTTT ATCCCTATAGCTCACAAGAGGCTATAGCCGTGGT CAAGATACACAACAATGATATAAAGGGTGCTACA GAGATATTACGTAGCCTGCTGAACGACAGGAAGT GCCCAATATTAATAAAAGCTAACGCGCAGGAAGT ACTTCGTATATACGGCTCTTGAAGAGCTTAGAGA CCGGTACTAGTTCCT	Twist Bioscience	N/A
Software and algorithms		
Proteome Discoverer v2.5	ThermoFisher Scientific	RRID:SCR_014477
Cytoscape 3.10	Cytoscape.org	RRID:SCR_003032
R (version 4.0.5)	R Core Team	https://www.r-project.org/
ggplot2	Wickham ¹³⁹	https://ggplot2.tidyverse.org/
Fiji	ImageJ	https://imagej.net/software/fiji/
AlphaFold-multimer	Cianfrocco et al. ¹⁴⁰	https://cosmic-cryoem.org/tools/alphafoldmultimer/
RCSB PDB Mol*3D Viewer	RCSB PDB	https://www.rcsb.org/3d-view
STRING	string-db.org	RRID:SCR_005223
Adobe Illustrator	Adobe	N/A
Other		
DAPI	Vector Laboratories	Cat#H-1200; RRID:AB_2336790
Imaging Spacer	Grace Bio-Labs	Cat#GBL654006
Low Protein Binding Collection Tubes (1.5 mL)	ThermoFisher Scientific	Cat#90410

EXPERIMENTAL MODEL AND STUDY PARTICIPANT DETAILS

Drosophila stocks

All stocks were grown and crosses performed on standard brown food made with blackstrap molasses.¹⁴¹ All flies were grown at 25°C with a 12-h light/dark cycle. Wild-type *wMel*-infected *D. melanogaster* flies were tetracycline-cured to generate uninfected *D. melanogaster* stocks.^{18,29} Similarly, *w-wRi*-infected *D. simulans* flies were tetracycline-cured to generate uninfected *D. simulans* stocks.^{136,137} Tetracycline curing occurred >5 years before experimentation, and infected and uninfected stocks were maintained in the lab for many years. The infection statuses of stocks were routinely tested using PCR with primers against the 16S rRNA gene of *Wolbachia*.¹³⁸

We obtained the following stocks from the Bloomington *Drosophila* Stock Center (BDSC): *Obp99b* deficiency (RRID:BDSC_25075); *fipi* deficiency (RRID:BDSC_9270); *Ilp5* mutant (RRID:BDSC_30884); *TfAP-2* deficiency (RRID:BDSC_8101); *mGluR* deficiency (RRID:BDSC_84132); *mGluR* RNAi (RRID:BDSC_25938). *elav-GAL4*¹⁴² (RRID:BDSC_458) was used to drive expression of *mGluR* RNAi in neurons. The *Wolbachia* infection status of these stocks was determined by PCR. If needed, flies with the correct genotype and infection status for use in experiments were created by crossing males from the stock to females from the wild-type infected or uninfected *D. melanogaster* stocks as required.

For all 10 × 10 crosses, 2-day old adult flies were used. Flies were either infected or uninfected with *Wolbachia* and male or female as indicated in the figures. The full genotypes of female flies used in the candidate genetic screen (Figure 5) were: *Obp99b* deficiency = w[1118]/w[1118]; Df(3R)BSC547/TM6C, Sb[1]; *fipi* deficiency = w[1118]/+; Df(2L)ED250, P{w[+mW.Scer\FRT.hs3] = 3'.RS5+3.3'}ED250/+; *Ilp5* mutant = w¹¹¹⁸/+; Tl[Tl]Ilp5¹/+; *TfAP-2* deficiency = w[1118]/+; Df(3L)ED4978, P{w[+mW.Scer\FRT.hs3] = 3'.RS5+3.3'}ED4978/+; *mGluR* deficiency = y[1] w[67c23]/+; Df(4)8-M318, P{w[+mW.hs] = hsp26-pt-Tj8-M318/+; and *mGluR* RNAi: *elav-Gal4/y[1] v[1]*; H2aV-RFP/+; P{y[+t7.7] v[+t1.8] = TRiP.JF01958}attP2/+.

Wolbachia-infected and uninfected female wild-type crawling third-instar larvae were used as the source of female larval brains for proteomics.

Wolbachia-infected and uninfected female wild-type crawling third-instar larvae were used as the source for female larval brain imaging.

Wolbachia-infected and uninfected female wild-type 2-7-day old adults were used as the source for female adult brain imaging.

Yeast

The yeast strain GHY2311 (*MATa his3Δ1 lys2Δ0 leu2Δ0 ura3Δ0 bar1Δ::NATMX*) was used for the expression of *Wolbachia* proteins in yeast. This strain is isogenic to S288C and is *GAL2+*. Frozen yeast stocks were streaked out onto a yeast peptone dextrose (YPD) plate at 30°C and grown for 2 days. Single colonies were then grown in YPD liquid media at 30°C overnight and were then transformed and plated on SC-leucine plate containing 2% glucose as described in.¹⁴³

METHOD DETAILS

10 × 10 progeny counts

Virgin male and female flies were collected immediately after eclosion and aged in groups for 2 days. Crosses were set up in standard bottles with 10 healthy male and 10 healthy female flies. Flies were randomly assigned to the appropriate crosses. After 7 days, all adults were removed and wandering 3rd instar larvae and pupae visible on the sides of the bottles were counted. After 5 more days, all adults that had emerged from each cross were counted. All aging and crosses were performed at 25°C with a 12-hour light/dark cycle.

Mating assays

Virgin male and female flies were collected immediately after eclosion and aged for 2 days in groups of 10 at 25°C with a 12-h light/dark cycle. Flies were aspirated into a 35 × 6 mm “mating chamber” and filmed for 1 h on the benchtop. Flies were randomly assigned to the appropriate crosses. Because some flies could become stuck in the food during aging or escape during transfer to the mating chamber, the number of copulations recorded was normalized to the number of female flies present in the mating chamber throughout the assay. The mating chamber was cleaned and dried between assays.

Sample preparation for microscopy

3rd instar female larval brains were dissected at room temperature in phosphate buffered saline (PBS). Brains were fixed for 20 min in 4% paraformaldehyde in 1 × PHEM buffer and blocked for 1 h in PBT (1 × PBS +0.05% Triton X-100 + 1% bovine serum albumin). Brains were stained with rabbit anti-FtsZ⁷⁴ (1:500) overnight at 4°C. After 3 × washes (15 min each) in PBT, brains were stained with anti-rabbit-Alexa488 (1:300 ThermoFisher Scientific A-11008) for 1 h at room temperature. Brains were washed 3 × (15 min each) in PBT and counterstained with DAPI in Vectashield (Vector Laboratories H-1200-10) before mounting.

Adult female brains were dissected in ice-cold PBST (PBS +0.5% Triton X-100). Brains were fixed for 30 min in 4% paraformaldehyde in PBS and then washed 4 × for >1 h in PBST before storing overnight at 4°C in PBST. The next day, brains were blocked for 1 h with PBST +5% goat serum, then stained with rabbit anti-FtsZ (1:250) and either mouse anti-nc82 (1:20 Developmental Studies Hybridoma Bank AB_2314866) or mouse anti-DoublesexDBD (1:10 Developmental Studies Hybridoma Bank AB_2617197) at 4°C for 12–48 h. Brains were washed 6 × (10 min each) in PBST then stained with anti-rabbit-Alexa488 (1:250) or anti-mouse-Alexa568 (1:250 Invitrogen A-11004) at 4°C for 12–48 h. Brains were washed 6 × (10 min each) in PBST, 1 × in PBS (10 min), and mounted in DAPI in Vectashield between a slide and coverslip separated with a spacer (Grace Bio-Labs GBL654006).

Confocal imaging

Larval and adult brain imaging was performed on an inverted Leica DMI6000 SP5 scanning confocal microscope. DAPI was excited with a 405 nm laser and collected from 410 to 480 nm. Alexa 488 was excited with a 488 nm laser and collected from 518 to 564 nm.

Alexa 568 was excited with a 543 nm laser and collected from 575 to 625 nm. Brains were imaged with either $\times 20/0.75$ or $\times 63/1.4$ oil objectives. Imaging was performed at room temperature. Images were acquired with Leica Application Suite Advanced Fluorescence software.

Sample preparation for mass spectrometry

3rd Instar female larval brain dissections were performed at room temperature in freshly prepared phosphate buffered saline (PBS). Each biological replicate consisted of 20 female brains. Excess PBS was removed from the samples, and dissected brains were snap frozen in liquid nitrogen before storing at -80°C . Each sample was thawed and then 25 μL of 5% SDS/50mM TEAB containing 50 mM dithiothreitol was added and samples were incubated for 10–15 min at 95°C . Samples were then spun again at 15,000 rpm for 15 min at 20°C and visually inspected to ensure no visible pellets were present. Supernatants were then removed and processed as described below.

Solubilized larval brain proteins were quantified using EZQ Protein Quantitation Kit (Thermo Fisher), and 14–16 μg of total protein alkylated using 40 mM final concentration freshly prepared iodoacetamide (Pierce) for 30 min in the dark at room temperature. Samples were processed using the S-trap Micro Columns (Protifi) following manufacturer's S-trap Ultra High Recovery Protocol. Briefly, samples ($\sim 30 \mu\text{L}$) were acidified to $\sim 1.2\%$ phosphoric acid by addition of a stock 12% phosphoric acid solution. Proteins were digested by addition of 2 μL of a 1 mg/mL solution of porcine trypsin (MS grade, Pierce) and layered onto the S-trap column containing 180 μL of 90% methanol/100 mM TEAB. Samples were briefly spun to remove excess buffer and washed $4\times$ with S-trap buffer. An additional 0.5 μg of trypsin and 25 μL of 50 mM TEAB was added to the top of each column and incubated for 1 h at 47°C . Samples were eluted off the S-trap columns using three elution buffers: 50 mM TEAB, 0.2% formic acid in water, and 50% acetonitrile/50% water +0.2% formic acid. Samples were dried down via speed vac and resuspended in 20–30 μL of 0.1% formic acid.

Liquid chromatography-tandem mass spectrometry

All LC-MS analyses were performed at the Biosciences Mass Spectrometry Core Facility (<https://cores.research.asu.edu/mass-spec/>) at Arizona State University. All data-dependent mass spectra were collected in positive mode using direct-injection into an Orbitrap Fusion Lumos mass spectrometer (Thermo Scientific) coupled with an UltiMate 3000 UHPLC (Thermo Scientific). One μL of peptides were fractionated using an Easy-Spray LC column (50 cm \times 75 μm ID, PepMap C18, 2 μm particles, 100 Å pore size, Thermo Scientific). Electrospray potential was set to 1.6 kV and the ion transfer tube temperature to 300°C . The mass spectra were collected using the "Universal" method optimized for peptide analysis provided by Thermo Scientific. Full MS scans (375–1500 m/z range) were acquired in profile mode with the Orbitrap set to a resolution of 120,000 (at 200 m/z), cycle time set to 3 s and mass range set to "Normal". The RF lens was set to 30% and the AGC set to "Standard". Maximum ion accumulation time was set to "Auto". Monoisotopic peak determination was set to "peptide" and included charge states 2–7. Dynamic exclusion was set to 60s with a mass tolerance of 10ppm and the intensity threshold set to 5.0e3. MS/MS spectra were acquired in a centroid mode using quadrupole isolation window set to 1.6 (m/z). Collision-induced fragmentation energy was set to 35% with an activation time of 10 ms. Peptides were eluted during a 240-min gradient at a flow rate of 0.250 $\mu\text{L}/\text{min}$ containing 2–80% acetonitrile/water as follows: 0–3 min at 2%, 3–75 min 2–15%, 75–180 min at 15–30%, 180–220 min at 30–35%, 220–225 min at 35–80% 225–230 at 80% and 230–240 at 80–5%.

Label-free quantification (LFQ)

We analyzed raw files searched against the Uniprot (www.uniprot.org) *Drosophila melanogaster* database (Dmel_UP000000803, fasta) using Proteome Discover 2.5 (Thermo Scientific). Raw files were searched using SequestHT that included Trypsin (specific) as enzyme, maximum missed cleavage site 3, min/max peptide length 6/144, precursor ion (MS1) mass tolerance set to 20 ppm, fragment mass tolerance set to 0.5 Da and a minimum of 1 peptide identified. Carbamidomethyl (C) was specified as fixed modification, and dynamic modifications set to Aceyl and Met-loss at the N terminus, and oxidation of Met. A concatenated target/decoy strategy and a false-discovery rate set to 1.0% was calculated using Percolator (25). The data was imported into Proteome Discoverer 2.5, and accurate mass and retention time of detected ions (features) using Minora Feature Detector algorithm. The identified Minora features were then used to determine area-under-the-curve of the selected ion chromatograms of the aligned features across all runs and relative abundances calculated. The mass spectrometry proteomics data have been deposited to the ProteomeXchange consortium via the PRIDE¹⁴⁴ partner repository with the dataset identifier PXD058588.¹⁴⁵

Gene ontology and PPI analyses

We performed gene ontology (GO) enrichment analyses using the website version of DAVID (v6.8) (26). We uploaded gene lists to DAVID (<https://david.ncifcrf.gov/tools.jsp>) and saved outputs for all three GO categories (BP, CC, MF) and associated statistical values. We used the default *D. melanogaster* gene list as background in DAVID to identify enriched GO terms associated the larval brain proteome (foreground $n = 8145$). ClueGO plugin v2.5.8 (27) for Cytoscape (v3.9.0) (28) was used to analyze differentially abundant proteins using the default *D. melanogaster* genome background to generate enriched GO categories using a right-sided hypergeometric test and P-values, adjusted using Benjamini-Hochberg for multiple testing correction. Enriched GO categories with false-discovery rate values below 1% are reported.

The differentially abundant protein identified by LFQ were interrogated for protein-protein interactions using STRING (<https://string-db.org/>). First, STRING was used to generate a complete network of all differentially abundant proteins using “high confidence (0.700)” criteria for inclusion and all disconnected nodes removed. The resulting PPI network was annotated to highlight subnetworks with specific cellular functions.

Predicting host-*Wolbachia* protein complexes with AlphaFold-multimer

AlphaFold-multimer predictions were generated using the COSMIC2 web-based gateway.¹⁴⁰ AlphaFold2 was used with the multimer parameter selected, which produced 5 scored models for each protein pair. *Wolbachia* effector protein sequences were accessed through the National Center for Biotechnology Information (NCBI) protein database.¹³⁵ mGluR (L0MPZ9) and Obp99b (D1FYT5) protein sequences were accessed through Uniprot. The highest scoring model for each *Wolbachia* effector-host protein pair was used to assess the potential complex. Complexes were viewed with the RCSB PDB Mol* 3D Viewer (<https://www.rcsb.org/3d-view>). The top-scoring.pdb files generated are available on Zenodo at <https://doi.org/10.5281/zenodo.14110800>.

Expression of *Wolbachia* proteins in yeast

The yeast expression assays are a modified version of the protocol described by.¹⁴⁶ The *Wolbachia* *WD_1127*, *WD_0295*, *WD_0523*, and *WD_1220* genes were codon optimized for expression in yeast and synthesized by Twist Bioscience (South San Francisco). These genes were inserted into pGH448, a centromeric, *LEU2* marked plasmid that uses the *GAL1* promoter to drive heterologous gene expression,⁷² using the New England Biolabs Golden Gate kit (New England Biolabs) according to the manufacturer’s instruction. The resulting plasmids were transformed into 10-beta competent *E. coli*.

Plasmids were isolated with the Nucleospin Plasmid EasyPure kit (Takara Bio) and transformed into the yeast strain GHY2311 (*MATa his3Δ1 lys2Δ0 leu2Δ0 ura3Δ0 bar1Δ::NATMX*). Transformed cells were grown to saturation in SC-leucine liquid media containing 2% glucose. These cells were counted, diluted to 1×10^7 cells/mL, 5-fold serial diluted, spotted to SC-leucine plates with either 2% glucose or 2% galactose as the carbon source, and incubated at 30°C for 2 days.

Simulations

Simulations were performed in R (4.0.5, R Core Team) and used measured mean and standard deviation values determined from the experimental mating assays performed in Figure 1F. For each generation, a random percentage of females (sampled from a normal distribution with the measured means and standard deviations) underwent mating. For simulations in which there was no difference in mating between infected and uninfected females, the percentages of mating females for each infection status were sampled from the same distribution (the measured uninfected mean and standard deviation). For simulations in which there was increased mating in infected females, the percentage of infected females mating was sampled from the distribution created with the infected mean and standard deviation while that of uninfected females was sampled from the distribution created with the uninfected mean and standard deviation. 100% of mated females produced progeny. Infected and uninfected females produced the same amount of progeny. The percentage of infected females out of all females was used to calculate the infection status of the population at each timepoint. Simulations were run for 50 generations. Each simulation was run 100 times, and the averages and standard error displayed. Code and associated data used for simulations is available on Zenodo at <https://doi.org/10.5281/zenodo.14058437>.

Experimental design

Specific sample sizes were not estimated before experimentation. Instead, all experiments were performed at least 3 independent times. Data were not blinded prior to analysis. No data were excluded from analysis. For experiments directly comparing different comparisons, experiments were performed during the same time period.

Figure preparation

Graphs were created in R with the ggplot2 package.¹³⁹ Images were adjusted for brightness and contrast in FIJI to improve clarity. Figures were created in Adobe Illustrator (Adobe, San Jose, CA, USA).

QUANTIFICATION AND STATISTICAL ANALYSIS

Independent runs of an experiment were considered technical replicates, and independent samples inside a single experimental run (e.g., stained brains) were considered biological replicates. Specific sample sizes were not explicitly determined prior to experimentation. Instead, each experiment was performed with at least three technical replicates. No outliers were excluded from analyses, and experiments were analyzed unblinded. Significance was defined as *p* value <0.05. Calculated *p* values for each statistical test can be found in the figures and are described in the figure legends. All statistical tests were performed in R. Kruskal-Wallis tests and Mann-Whitney tests were selected to compare distributions with no assumption of normalcy. For experiments testing specific hypotheses (Figures 1E, 1F, 5D–5G, S4A, and S4D), one-sided tests were performed in the direction dictated by the hypothesis. Two-sided tests were performed otherwise. A two-sided Fisher test was performed with a 2×2 contingency table for Figure 1G. The definitions of *N* can be found in the figures. For all 10×10 assays (Figures 1B, 1C, 1H, 1I and 5D–5H), *N* = the number of independent 10×10 crosses performed. For direct analysis of mating (Figures 1E–1G), *N* = number of copulations observed (Figure 1E), *N* = of independent assays

performed), and n = total number of female flies observed. Data are presented as box and whisker plots (median \pm upper and lower quartiles) with all individual values plotted. Simulations of the spread of *Wolbachia* through a population are presented as the mean $\pm 2 \times$ SEM.

ADDITIONAL RESOURCES

Proteomics data are deposited to the ProteomeXchange consortium via the PRIDE partner repository at ProteomeXchange::PXD058588.

Code and associated data used for simulations is available on Zenodo: <https://doi.org/10.5281/zenodo.14058437>.

The top-scoring.pdb files of potential *Wolbachia* effectors with mGluR and Opb99b generated are available on Zenodo: <https://doi.org/10.5281/zenodo.14110800>.